



Observed trends and coherent changes in daily rainfall extremes over Greater Mumbai, 1985–2020

Rohit Mann¹ · Anju Gupta¹ · Amit Dhorde² · Swati Sharma¹

Received: 15 July 2022 / Accepted: 29 December 2022 / Published online: 14 January 2023
© The Author(s), under exclusive licence to Springer-Verlag GmbH Austria, part of Springer Nature 2023

Abstract

Climate extremes are predicted to become more frequent and severe in the future, owing to rising greenhouse gas emissions in the atmosphere. Using appropriate trend indices, this study intends to analyze the effects of climate change on rainfall variability and extreme rainfall events in the millennium city of Mumbai. The analysis was carried out for the period 1985–2020 for 2 stations and 23 stations were selected (2006–2020) later from the dense rain gauge network of Municipal Corporation of Greater Mumbai (MCGM). To comprehend the trend and behaviour of rainfall and extreme events, three statistical models were used: Mann–Kendall test, Sen’s slope estimator, and simple linear regression; for abrupt change point detection, Pettitt’s test, standard normal homogeneity test, Buishand’s range test, and von Neumann ratio test were used. The results indicated that average annual rainfall in the study area is 2208.82 mm which is increasing at the rate of 5.18 mm/year (at 99% confidence level). The frequency of heavy (> 120 mm/day) and extreme heavy rainfall events (250 mm/day) increased over Santacruz after 1994 and in the case of Colaba, it increased after 2005. The examination of rainfall and temperature data series for abrupt change point identification suggests that several change points exist, with the highest change points occurring between 2001 and 2005. Extreme climate event scenarios shown here could have large-scale negative consequences for the ecosystem and ecological resources of the study area.

1 Introduction

Using widely available long-term monthly time series data, a great deal of effort has been done in the last three decades evaluating changes in monthly precipitation and mean maximum, minimum, and average temperature for so many parts of the world (e.g. Easterling et al. 1997; Peterson and Vose 1997; Hansen et al. 2001; New et al. 2001; Jones and Moberg 2003). Changes in monthly values, on the other hand, address only a small fraction of issues related

to climate variability and climate change. Frequent changes in weather extremes have substantial impacts than alterations in average value. Moreover, shifts in anomalies can be potent markers of climate change, as it has been postulated that the hydrological cycle will be more active in a warming world in which the atmosphere can retain more water vapour (Folland et al. 2001). A “world—wide” evaluation of shifting climatic extremes published in 2002 (Frich et al. 2002) did not use data from Central or South America and only a tiny quantity from Africa and southern Asia. Different studies were conducted in all over the world by using monthly and daily data of both rainfall and temperature which revealed interesting results. Researchers conducted studies based on a set of parameters showing the increase in both precipitation and temperature in different parts of the world, e.g. central and northern South America (Aguilar et al. 2005), central and south Asia (Klein Tank et al. 2006), South America (Vincent et al. 2005), Canada (Vincent and Mekis 2006), southeast Asia and south Pacific (Manton et al. 2001), Western US (Hamlet et al. 2005), India (Pal and Al-Tabbaa 2010), South America (Haylock et al. 2006), Australia (Haylock and Nicholls 2000), Argentina (Rusticucci and Barrucand 2004), China (Zhai et al. 2005), South Asia

✉ Rohit Mann
mannrohit96@gmail.com

Anju Gupta
anjugupta172@gmail.com

Amit Dhorde
amitdhorde@gmail.com

Swati Sharma
Swatisharmaraina@gmail.com

¹ Department of Geography, Kurukshetra University, Kurukshetra, India

² Department of Geography, Savitribai Phule Pune University, Pune, India

(Gunnell 1997), and Caribbean region (Peterson et al. 2002). Furthermore, different patterns are observed in the study of Europe by Klein Tank and Konnen (2003). They investigated precipitation and temperature trends from 1946 to 1999 and divided the time period in two halves, i.e. 1946–1975 and 1976–1999. In the case of temperature, decrease in warm extremes was observed in first half but, in the second half, the increase in the rate of temperature doubled. Throughout the time period, precipitation showed an increasing trend over Europe. In his study, Frich et al. (2002) evaluated daily data and found that throughout the second half of the twentieth century, the worldwide land area was more affected by a major change in climatic extremes. Also, world patterns of precipitation and temperature were studied by Alexander et al. (2006) and found that over 70% of the land in the world exhibited a significant drop in annual cold night occurrence and a substantial increase in yearly warm nights. He also observed changes in precipitation and demonstrated widespread and dramatic increase in precipitation, but the changes were significantly less spatially coherent than the changes in temperature.

Apart from the above studies, several studies were also conducted on different coastal and mega cities all around the world. These studies measure the impact of rainfall variability on climate change. Some studies conducted by different scholars are Emery and Aubrey (1991), Roth (2000), Buytaert et al. (2006), Carrera-Hernandez and Gaskin (2007), McGranahan et al. (2007), Nicholls et al. (2008), World Bank (2010), and Hanson et al. (2011). Emery and Aubrey (1991) conducted the study by taking into account the parameters of glacial rebound and relative Sea Levels in Europe from Tide-Gauge records. The results of his study find that rise in sea level in different parts of the European coast due to melting of ice sheets as a result of atmospheric warming. Roth (2000) investigated more than fifty studies in his review of atmospheric turbulence over cities and reported that increasing tendencies in climatic extremes were observed in most of the studies. Also, Buytaert et al. (2006) and Carrera-Hernandez and Gaskin (2007) studied the spatio-temporal patterns of rainfall and temperature over south Ecuadorian Andes and Mexico Basin. The results of both the studies reveal that rainfall variability is extremely high especially in the case of mountain environment over Ecuadorian Andes. Apart from that, Nicholls et al. (2008), Hanson et al. (2011), and World Bank (2010) investigated the estimate exposure of the world's large port cities with reference to climatic extremes. The results revealed that the most significant global drivers of the total rise in exposure, particularly in emerging nations where low-lying areas are urbanized, are population expansion, socio-economic growth, and urbanization. Furthermore, McGranahan et al. (2007) signify the assessment of the Impacts of Climate Change and Human Settlements in Low Elevation Coastal

Zones. This study reveals that they carry out the first global analysis of the population and urban settlement patterns in the Low Elevation Coastal Zone (LECZ), which is here defined as the continuous area along the coast that is less than 10 m above sea level. This region is home to 10% of the world's population and 13% of the world's urban population, although only making up 2% of the world's land area. Also, different researchers analyze the spatio-temporal patterns of precipitation. For example, Liuzzo et al. (2015) conducted a deep investigation of rainfall patterns over Sicily from 1921 to 2012. Data on precipitation showed that Sicily experienced a general decline in precipitation from 1921 to 2012. During the fall and winter, downward trends were prevalent. However, between 1981 and 2012, there was a discernible rise in the amount of precipitation that fell annually. Recent temporal trends of precipitation and temperature over Langkat River Basin, Selangor, Malaysia, is studied by Amirabadizadeh et al. (2015). The analytical findings showed that, while there were increasing and decreasing trends in the annual and seasonal precipitation and temperature, only the increasing trends were significant at the 95% confidence level. The relationship of rainfall and river discharge variations over Southwestern Iran from 1956 to 2012 was studied by Sabzevari et al. (2015). The results of the precipitation time series showed that the majority of the stations had insignificant trends in both the annual and monthly series. When discharge trends were analyzed, it was discovered that both the annual and the October through April series had a significant rise. Interestingly, monthly precipitation trends over Iran (Khalili et al. 2015; Asakereh 2016) and modelling of monthly rainfall and runoff relationship over Urmia Lake Basin, Iran, were studied by Farajzadeh et al. (2014) and Fathian et al. (2016). The results of the PCI index showed a significant increasing trend in the data, indicating significant increase of precipitation concentration abnormalities all over Iran. Whereas the amount of annual precipitation declined from southwest to northeast, it was concentrated in the southwest and in mountainous areas. However, the temporal trends in precipitation over Urmia Lake Basin demonstrated that over the basin, both increasing and decreasing patterns were apparent at all-time scales. Also, spatial patterns of rainfall over Bangladesh and Greece were studied by Bari et al. (2016) and Markonis et al. (2016) respectively. Spatio-temporal trends of rainfall over Bangladesh exhibited declining trend in annual rainfall values over western, north-western, south-central, south-western, north-eastern, and northern part of northern region whereas rising trend is found only in south-eastern region. In the case of Greece, trends in rainfall exhibit an increasing trend.

Heavy rainfall has serious ramifications for modern civilization. Changes in the severity and frequency of weather extremes will most likely be felt as a result of climate change (Sarker 1966; Venkatesh and Jose 2007; Dhorde et al. 2009;

Ratna 2012). As per studies, anthropogenic activities have contributed to a rise in atmospheric greenhouse gas concentrations, which has resulted in the strengthening of heavy rainfall events (Bussi eres and Hogg 1989; Kulkarni and Reddy 1994; Narkhedkar et al. 2006; Kothawale et al. 2010). Across different locations round the world, the severity of heavy rainfall events is poised to increase as a result of global warming (Ashrit et al. 2001), even in locations where average rainfall is decreasing (e.g. Semenov and Bengtsson 2002; Wilby and Wigley 2002). Thus, as a result of these high rainfall events, it is imperative to understand the associated hydrological risk that helps in building of urban infrastructure designs (Ramachandran and Banerjee 1983; Korade and Dhorde 2016). Indian economy is primarily based on agriculture. Therefore, assessing the variability of rainfall across India is really a significant task. Many studies in this regard are conducted by different researchers, particularly dealing with spatio-temporal patterns of rainfall and temperature in different states across India (Mondal et al. 2015, 2018; Chandniha et al. 2016; Jin and Wang 2017; Prabhakar et al. 2017; Nema et al. 2018; Warwade et al. 2018; Pal et al. 2019; Pillai et al. 2019). These studies basically address the trends and patterns of precipitation with reference to climate change. Since majority of the population lives in cities, a change in extreme storm events might have a significant influence on India's booming economy. Since the turn of the twentieth century, several researchers have examined rainfall trends in India. Parthasarathy et al. (1993), Roy and Balling (2004), and Rana et al. (2012), among several others, have explored the long-term tendencies in southwest monsoon over India. Long-term trends show a significant decline in the probability of moderate-to-heavy rainfall events in most parts of India (e.g. Naidu et al. 1999; Dash et al. 2009). This is endorsed by a considerable rise in the incidence and intensity of monsoon breaks over India in past few decades (Kripalani et al. 2003; Ramesh Kumar et al. 2009; Turner and Hannachi 2010), and perhaps an increased prevalence of heavy rainfall events (100 mm/day) in certain parts of the state (Gadgil 1986; Goswami et al. 2006). Scientific research for India based on climatic model simulations implies that greenhouse gas-induced climate change will substantially boost monsoon rainfall across a vast region spanning South Asia (e.g. Lal et al. 2000; May 2002, 2004, 2011; Rupakumar et al. 2006). However, due to substantial discrepancies in model projections, accurate projection of future developments in regional monsoon rainfall has raised questions (e.g. Kumar et al. 2011; Sabade et al. 2011). Models based on climate show that the reaction of rainfall to global warming is coupled with a reduction in southwest monsoon (e.g. Kripalani et al. 2003; Ueda et al. 2006; Sabade et al. 2011; Krishnan et al. 2013; Stowasser et al. 2009). Nevertheless, Rupakumar et al. (2006) evaluated the consequences of climate change in India by

reviewing the PRECIS climate model by using present-day simulation (1961–1990) and found that a slight increase in intense rainfall events along the west coast (Patwardhan and Asnani 2000; Tawde and Singh 2015) and western regions of central India.

Multiple researchers have examined Mumbai's vulnerability to long-term climate scenarios. Increase in anthropogenic activities and greenhouse gases may exacerbate the problem of urbanization pressures in the coming decades. Bohra et al. (2006), Ranger et al. (2011), and Hallegatte et al. (2013) painted a bleak image of Mumbai flooding and the associated financial damage during the floods of 26 July 2005, and then went on to examine the problem in possible conditions. The interplay of multispectral weather systems with macro-scale coastal land-surface features, as well as inadequate rainfall size, extent, and intensity predictions by existing weather-forecast models, may be the root causes of such rainfall vagaries (Jenamani et al. 2006; Shyamala and Bhadram 2006; Lei et al. 2008; Chang et al. 2009; Zope et al. 2015). They hypothesized that the development of a macro level vortex over Mumbai and the interplay of multi-temporal weather systems with meso-scale coastal land-surface features contributed to the intensification of this extremely confined rain event. Following the occurrence of the heavy rain event on 26 July, IMD in Mumbai realized how inadequate it was to have only two rainfall-recording meteorological stations (at Santacruz and Colaba). In order to record the spatial pattern of rainfall in Mumbai, the Municipal Corporation of Greater Mumbai (here after uses as MCGM) planned to establish 26 rain gauging stations in the city in 2006 which later increased to 60 (MCGM 2007; Lokanadham et al. 2009).

For rainfall events exceeding 25 mm/h, Nikam and Gupta (2013) developed a forecasting methodology that combined the probabilistic global search-Lausanne (PGSL) and least-squares support vector machine (LS-SVM) techniques. However, this method was unable to clearly capture spatio-temporal variability. Furthermore, efforts have been made to estimate the rainfall design for Mumbai along with such studies on rainfall forecasting. Sen et al. (2013) used 43 years (1969–2012) of rainfall data in Mumbai to perform at-site design storm estimation for two rain gauge stations (Santacruz and Colaba) in order to quantify its spatio-temporal variability. Using the same dataset, Sherly et al. (2015) proposed a methodology for rainfall design and estimation using a multivariate semi-parametric approach. The present research work is one of the few studies that use data from Indian Meteorological Department (IMD), disaster department, and MCGM to evaluate the rainfall variability and possible impacts of heavy storm events in the study area. Such potential consequences might have major ramifications for Mumbai, i.e. India's financial capital. Throughout this investigation, it was examined that how in the metropolis

of Greater Mumbai (consists of city and sub-urban district), deviations in rainfall dataset have changed as a result of climate change. Therefore, the main objective of the present research work is to apply various statistical tests in order to understand the behaviour of rainfall trends and extreme events.

2 Study area

In Western Ghats, Mumbai is among the most prominent megacity and a big coastline (Fig. 1). It spans from 18°53'N to 19°16'N latitude, and from 72°E to 72°59'E longitude, covering an area of 471.9 sq. km. Mumbai is the world's fifth most populous megacity, with a population density of 4445 people per square kilometer (Census of India 2011; United Nations 2012). In the metropolitan city of Mumbai, prominent geomorphological features are also found like rivers, water bodies, canals, creeks,

linear ridges, terrestrial harbours, and coastal lowlands. Peninsular Mumbai is known for its numerous medium and small islands, reclamation sites, and drainage features. The Creek of Thane in the east and the Arabian Sea in the west define the city of Mumbai on India's western coast. During the southwest monsoon, the area receives an average rainfall of about 253.3 cm of rain per year (1990–2015), with July and August accounting for almost 90% of this total. The annual mean temperature remains between 27.2 and 28.8° C and the city's relative humidity ranges from 54.5 to 85.5% (IMD 2007). The Mumbai city's tidal height ranges around 1.8 to 3.5 m. Tidal flushing in the city's lower reaches is a sign of rising sea levels (GRB Report 2006, 2013). Forests, mangroves, wetlands, and lakes are all part of the city's natural landscape. In the study area, coastal mangroves and wetlands have a key role in preventing coastal erosion (Dahdouh-Guebas et al. 2005; GRB Report 2006; Pacione 2006).

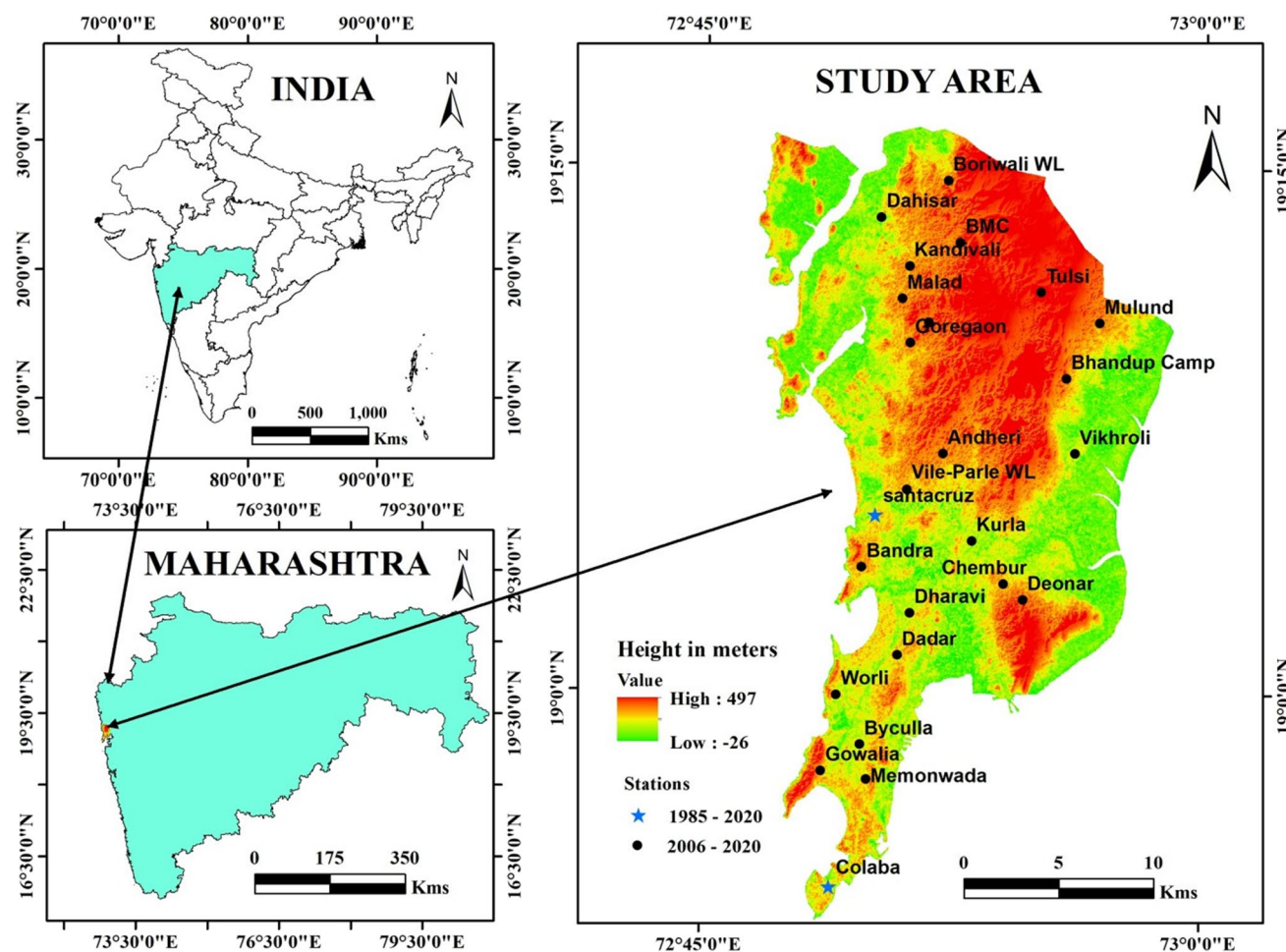


Fig. 1 Locational map of the study area along with its rain gauge stations

3 Database and methodology

3.1 Data collection and composition

Hourly data of rainfall and temperature for 2 stations, i.e. Colaba and Santacruz setup by IMD, which represent the city district and sub-urban district respectively, are used in the present study (1985–2020). Later, a dense network of rain gauge stations (60 stations at present) was set up by Disaster Department, MCGM after the heavy storm event of 26 Jul, 2005. The current study selects a total of 23 stations out of 60 (MCGM 2007) and use data that was obtained from MCGM (2006–2020). The stations are selected by using a distance matrix tool in ARC GIS 10.9. The dense network of selected stations is shown in Fig. 1.

General information of each selected station like coordinates, mean annual rainfall, annual maximum, and minimum rainfall with their respective years is shown in Table 1. Also, station-wise general information based

on daily statistics like daily maximum rainfall with their respective year, SD, and CV is shown in Table 2. The climate data were subjected to trend analysis after homogeneity and homogenization were checked. Monthly, seasonal, and annual time series are created by averaging daily values. The IMD has designated four seasons: (a) winter (January–February), (b) pre-monsoon (March–May), (c) monsoon (June–September), and (d) post-monsoon (October–December). Though this paper primarily focuses on rainfall variability and extreme events, analysis of temperature has also been carried out as both rainfall and temperature are co-related to each other.

3.2 Methodology

For each station, appropriate statistical methodologies such as summation, average, percentage, standard deviation (SD), coefficient of variation (CV), skewness (C_s), kurtosis (C_k), and moving average were performed. The

Table 1 General information of Selected Stations in the study area based on annual statistics (2006–2020)

Sr no	Station	Latitude	Longitude	Mean rainfall (mm)	Maximum		Minimum		S.D (mm)	CV (%)	C_k	C_s
					Rainfall (mm)	Year	Rainfall (mm)	Year				
1	Santacruz (1985–2020)	19.0843	72.836	2306.55	3721.99	2020	1287.25	1986	564.61	24.48	2.85	1.81
2	Colaba (1985–2020)	18.9067	72.8147	2111.09	3511.35	2020	1229.8	2002	540.89	25.62	2.62	1.79
3	Andheri	19.1136	72.8697	1774.77	2604.13	2011	1042.71	2015	470.81	26.53	-0.698	1.97
4	Bhandup Camp	19.1499	72.9311	1827.68	2639.36	2007	1083.35	2015	471.66	26	-0.79	1.85
5	Bandra	19.0596	72.8295	1737.12	2621.62	2011	1015.34	2015	469.11	27	-0.55	2.09
6	Boriwali WL	19.2381	72.8523	1775.02	2615.08	2007	1039.02	2015	480.4	27.06	-0.77	1.92
7	Byculla	18.975	72.8295	1732.29	2626.39	2011	1014.03	2015	461.52	26.64	-0.49	2.11
8	Chembur	19.0522	72.9005	1791.96	2620.63	2011	1057.3	2015	466.31	26.02	-0.68	1.96
9	Dadar	19.0178	72.8478	1746.85	2632.82	2011	1024	2015	466.27	26.69	-0.53	2.09
10	Deonar	19.0447	72.9103	1798.68	2622.42	2011	1062.6	2015	465.57	25.88	-0.69	1.95
11	Dharavi	19.038	72.8538	1753.73	2626.76	2011	1028.65	2015	467.01	26.63	-0.57	2.06
12	Gowalia	18.9623	72.8101	1717.55	2619.526	2011	1133.92	2018	459.96	26.78	-0.46	2.13
13	Kurla	19.0726	72.8845	1781.74	2615.36	2011	1193.21	2018	467.86	26.26	-0.68	1.96
14	Malad	19.1874	72.8484	1766.32	2577.37	2007	1195.96	2018	476.71	26.99	-0.74	1.95
15	Mulund	19.1765	72.9475	1844.05	2674.56	2007	1257.94	2018	473.37	25.67	-0.81	1.81
16	Vikhroli	19.1142	72.9358	1827.03	2600.51	2011	1235.81	2018	469.09	25.68	-0.76	1.87
17	Vile-Parle WL	19.0968	72.8517	1758.65	2609.91	2011	1030.71	2015	470.36	26.75	-0.65	2.01
18	Worli	18.9986	72.8174	1721.37	2638.33	2011	1005.46	2015	466.45	27.09	-0.42	2.12
19	Tulsi	19.191	72.918	1822.31	2653.22	2007	1078.27	2015	475.09	26.07	-0.8	1.85
20	Dahisar	19.4946	72.8604	1810.43	2793.88	2007	1273.41	2018	505.28	27.91	-0.73	1.83
21	Dindoshi	19.1762	72.8617	1775.52	2583.96	2007	1041.48	2015	475.32	26.77	-0.74	1.94
22	Goregaon	19.1663	72.8526	1766.68	2589.87	2011	1193.4	2018	475.08	26.89	-0.72	1.96
23	Kandivali	19.2029	72.8518	1770.71	2591.22	2007	1036.71	2015	477.7	26.98	-0.75	1.94
24	Memonwada	18.9585	72.8329	1736.18	2618.47	2011	1017.13	2015	458.44	26.41	-0.53	2.06
25	BMC	19.2143	72.8771	1826.04	2360.39	2020	1089.49	2015	388.05	21.25	-0.66	1.4

SD standard deviation, CV coefficient of variation, C_k kurtosis, C_s skewness

Table 2 General information of selected stations in the study area based on daily statistic of monsoon season (2006–2020)

Sr no	Stations	Maximum		Monsoon season	
		Rainfall (mm)	Year	SD (mm)	CV (%)
1	Santacruz (1985–2020)	944	2005	207.36	39.78
2	Colaba (1985–2020)	1058.9	2011	161.08	34.26
3	Andheri	204.8	2020	66.03	15.57
4	Bhandup Camp	177	2009	68.72	15.75
5	Bandra	261.1	2020	65.35	15.76
6	Boriwali WL	302.6	2011	65.51	15.36
7	Byculla	203.1	2020	65.62	15.90
8	Chembur	232.1	2012	67.46	15.83
9	Dadar	233.1	2011	66.47	15.98
10	Deonar	231.2	2011	67.84	15.87
11	Dharavi	228.9	2020	66.27	15.86
12	Gowalia	202.1	2019	64.85	15.83
13	Kurla	203.2	2020	67.41	15.90
14	Malad	217.2	2018	62.77	14.75
15	Mulund	285.8	2011	70.60	16.05
16	Vikhroli	220.9	2015	70.81	16.32
17	Vile-Parle WL	202.1	2011	66.45	15.84
18	Worli	226.9	2019	64.96	15.79
19	Tulsi	250.2	2017	68.60	15.74
20	Dahisar	293.5	2011	71.65	16.29
21	Dindoshi	198.9	2011	64.34	15.09
22	Goregaon	313.2	2011	64.93	15.33
23	Kandivali	212.4	2011	65.42	15.40
24	Memonwada	199.3	2019	65.22	15.77
25	BMC	173.2	2017	65.85	15.68

SD standard deviation, CV coefficient of variation

extreme storm event was then estimated using the procedure outlined below.

3.2.1 Identification of heavy and extreme heavy rainfall events

To examine rainfall climatology and analyze various categories of extreme rainfall events, criteria given by IMD were

Table 3 Various categories of rainfall events and respective rainfall intensity ranges as defined by India Meteorological Department (IMD)

Figure 1 Locational map of the study area along with its rain gauge stations	Figure 1 Locational map of the study area along with its rain gauge stations
Very light rain (VLR)	Trace–2.4
Light rain (LR)	2.5–15.5
Moderate rain (MR)	15.6–64.4
Heavy rain (HR)	64.5–115.5
Very heavy rain (VHR)	115.6–204.4
Extremely heavy rain (EHR)	> 204.4

Source: IMD 2021

used, which are as follows: very light rainfall (VLR), light rainfall (LR), moderate rainfall (MR), heavy rainfall (HR), very heavy rainfall (VHR), and extremely heavy rainfall (EHR). Table 3 depicts different rainfall intensity ranges for various IMD-classified rainfall events. In this study, extreme rainfall event is categorized as very heavy (115.6–204.4 mm/day) and extremely heavy (> 204.5 mm/day) based on the rainfall intensity and IMD criteria of defining heavy rainfall events. Very heavy and extremely heavy rainfall events are calculated by taking into account the highest rainfall in a year on a certain day. The list of very heavy and extremely heavy rainfall events is calculated manually by the authors.

3.2.2 Trend detection

To discover the trends in rainfall and temperature datasets, statistical approaches such as the Mann–Kendall test (Mann 1945; Kendall 1948), Sen's slope estimator (Sen 1968), and simple linear regression were applied. The non-parametric rank-based Mann–Kendall is an outstanding tool for determining trends in time series data at various meaningful intervals (Singh et al. 2015). The trend and its significance level are determined using the standard normal variable Z . Positive Z values indicate an upward trend, whereas negative ones indicate downward trend. The value of Z for a 95% confidence level of 1.96 was used in the current study. When the value of Z in both the rainfall time series is greater than 1.96, it indicates a substantial increasing or decreasing trend. The current study uses Sen's slope estimator to determine the trend's intensity. If a dataset has a linear trend, the slope of the trend (change per unit time) can be correctly predicted (Sen 1968). The trend in a temporal dataset is also detected by using parametric simple linear regression. The approaches outlined above are commonly utilized in hydro-meteorological investigations to discover trends.

3.2.3 Homogeneity analysis

There are different ways to evaluate the inhomogeneity or abrupt change point in a data series. These techniques can be broadly divided into relative and absolute (Yang et al. 2018). The inhomogeneity of the dataset is

separately evaluated using the absolute methods across each station without taking data from neighbouring stations into account. Through the use of neighbouring station data, inhomogeneity within a time series is found by using relative approach (Ahmed et al. 2018; Ahmed et al. 2021). Comparing the spatial and temporal variation of chosen series to the nearby series reveals that the relative approach is more trustworthy. Despite the fact that relative approach is the more effective, Yozgatligil and Yazici (2016) suggested that their effectiveness is highly dependent on the caliber of the data from the nearby stations. Additionally, relative techniques are inappropriate for the region where stations are spaced. However, each station has a different topography and environment, making it challenging to identify a strong relationship with other stations. So, wherever possible, absolute procedures are preferred against relative ones. Finding the best absolute homogeneity strategy for a given situation is never easy because there are so many different options available. Since each approach has merits and demerits. Therefore, using a variety of techniques to check the homogeneity or abrupt change point of data for a particular area is generally advised (Singh et al. 2019). Detecting abrupt change point in a time series is critical for determining the period during which significant change occurred. The next sections go through the specifics of many abrupt change point detection tests used in the study.

Pettitt’s test The non-parametric Pettitt’s test is helpful in detecting sudden change in a time series dataset (Winingaard et al. 2003). It also detects a big shift in the mean of a time series when the period of the alteration is uncertain. If $x_1, x_2, x_3, \dots, x_n$ is actually a series of observable data with a deviation at t , then $x_1, x_2, x_3, \dots, x_t$ have a distribution function $F_1(x)$ that differs from the distribution function $F_2(x)$ of the second segment of the series $x_{t+1}, x_{t+2}, x_{t+3}, \dots, x_n$, then Pettitt’s (1979) test is true. The mathematical expression for this test statistic (U_t) is:

$$U_t = \sum_{i=1}^t \sum_{j=t+1}^n \text{sgn}(x_i - x_j) \tag{1}$$

$$\text{sgn}(x_i - x_j) = \begin{cases} +1, & \text{if } (x_i - x_j) > 0 \\ 0, & \text{if } (x_i - x_j) = 0 \\ -1, & \text{if } (x_i - x_j) < 0 \end{cases} \tag{2}$$

where x_i signifies date value at time i .

For the sample length (n), the test statistic K and the accompanying confidence level (q) can be defined as:

$$K = \text{Max}|U_t| \tag{3}$$

$$p = \exp\left(\frac{-K}{n^2 - n^3}\right) \tag{4}$$

Whenever q is below the specified confidence threshold, null hypothesis is rejected. The projected significance probability (P) for a change point is defined as:

$$P = 1 - p \tag{5}$$

where there is a significant dramatic change point, the series is clearly separated into two sub-series at that time. At various confidence levels, the test statistic K can be compared to the corresponding statistic for detecting a transition point in a time series. This test is commonly used to detect changes in hydrological and climatological investigations (Zhang et al. 2008; Guerreiro et al. 2014).

Standard normal homogeneity (SNH) test The time series (T_t) is separated into two portions for the SNH test (Alexanderson 1986), one from 1 to t years (z_1) and the second from t to $n-t$ years (z_2). Then, by using following mathematical statement, the averages of these two series are compared:

$$T_t = tz_1^2 + (n - 1)z_2^2 \tag{6}$$

where z_1 and z_2 are calculated as follows:

$$z_1 = \frac{1}{t} \sum_{i=1}^t \frac{(x_i - \bar{x})}{\sigma x} \tag{7}$$

$$z_2 = \frac{1}{n - 1} \sum_{i=t+1}^n \frac{(x_i - \bar{x})}{\sigma x} \tag{8}$$

where the standard deviation and mean of the time series are σx and \bar{x} respectively. The year t is a turning point, with a break where the value of T_t reaches its highest peak. The test statistic must be greater than the crucial value to reject the null hypothesis, which is determined by the sample size (n).

Buishand range test This is indeed a non-parametric test that can be used with variables of any distribution (Buishand 1982). The observed time series are thought to be distinct of one another. The test statistic B_t is calculated as follows:

$$B_t = \sum_{i=1}^t (x_i - \bar{x}) \tag{9}$$

Even though the time series is evenly distributed around its average value on both sides of the mean series, it can be homogenous without any change points if $B_t=0$. The rescaled adjusted range (R) can be used to determine the importance of the shift.

$$R = \frac{\text{Max}(B_t) - \text{Min}(B_t)}{\bar{x}} \quad (10)$$

Von Neumann ratio test This test detects heterogeneity in any time series that is not expressed as a tight stepwise shift. Furthermore, Jaiswal et al. (2015) found that this test is highly related to the first-order serial correlation coefficient. The parameter N_e of the test is expressed as the time series variance divided by the mean square successive difference and is denoted as:-

$$N_e = \frac{\sum_{i=1}^{n-1} (x_i - x_{i-1})^2}{\sum_{i=1}^n (x_i - \bar{x})^2} \quad (11)$$

Following the Winingaard et al. (2003) technique, rainfall and temperature data series of a station are classified as homogenous (no change point) if none or one of the four tests contradicts the null hypothesis at a 5% significant level. If two out of four tests reject the null hypothesis at a 5% significant level, a station's rainfall and temperature time series is considered heterogeneous (doubtful), and if more than two tests reject the null hypothesis at a 5% significant level, the rainfall all over Mumbai is considered heterogeneous. Various research papers suggest that Pettitt's test is more reliable in detection of abrupt change point in a data series.

4 Results and discussion

4.1 Annual analysis

For the entire duration of time-series data, Table 1 shows the distribution of climatological mean, maximum, and minimum rainfall. Dataset exhibits the maximum rainfall (2306.55 mm) over Santacruz and the minimum rainfall (1717.55 mm) over Gowalia, with SD values ranging from 388.05 to 564.61 mm. Furthermore, the year 2020 has recorded the highest rainfall (3721.99 mm) and the least in 2015 (1005.46 mm). It was observed, the years 2007, 2011, and 2020 are the years of maximum rainfall and 1986, 2002, 2015, and 2018 were the years of minimum rainfall. It is clearly seen from the analysis that the rainfall deficit years coincide with the El Nino years. Both C_S and C_K are the indicators of data flatness, unevenness, distortedness, symmetry (or, more correctly, lack of symmetry), and their values for a normal data distribution are close to zero. In a normal distribution, C_K determines whether data is heavy-tailed or light-tailed, whereas C_S determines whether a dataset is symmetric or asymmetric. Santacruz and Colaba stations in the study area have high C_K , but Mulund has a low C_K . Except for Colaba and Santacruz, all of the stations

show a negative C_S , indicating that rainfall is falling over the rest of the stations while increasing over Colaba and Santacruz.

The spatial distribution of normal annual rainfall and CV from 1985 to 2020 is constructed (Fig. 2a, b). The map shows that rainfall has little variations in its spatial distribution. It is high over Santacruz and BMC stations and low over Bandra, Dharavi, Dadar, Worli, Byculla, Memonwada, and Gowalia (Fig. 2a). In the case of CV, the values are high in city and northern part and low over Colaba, Santacruz, and BMC stations (Fig. 2b). As per Hare (2003), CV is being used to categorize rainfall occurrences into three categories: low ($CV < 20$), moderate ($20 < CV < 30$), and high ($CV > 30$). According to the above-cited paper, the study area falls in the moderate variability zone. The CV values in the study area decrease around Santacruz and BMC station, indicating that variability is high in the rest of Mumbai. Its proportions drop from 27.91% in Dahisar to 21.25% in BMC (Fig. 2b). Figures 3 and 4 show the distribution of rainfall and average annual temperature over the stations that are setup by BMC. From the bar and line graphs, it is clearly seen that rainfall has decreased in all stations, whereas it has increased over Santacruz and Colaba (Fig. 5). Apart from this, the temperature values have also increased. This differential behaviour of monsoon around Mumbai is influenced by variety of factors like the impact of Western Ghats or Sahyadri Mountains (which stretch across the states of Maharashtra, Karnataka, and Kerala) on monsoon winds around Mumbai. When the Somali Jet, which are powerful winds of the southwest monsoon, carrying moist air from the Arabian Sea collides with the Western Ghats, they are orographically lifted (Jenamani et al. 2006). A number of other phenomena, such as the existence of a meso-scale offshore vortex over the northeast Arabian Sea and the north-westward passage of low-pressure systems from the Bay of Bengal via the monsoon trough, also contribute to this erratic behaviour of monsoon in and area around Mumbai. The heavy rainfall event on July 26, 2005, in Mumbai clearly proves that variability in rainfall is high as rainfall values across different stations are highly variable. This intensely localized rainfall event that occurred over a 24-h period in several parts of Mumbai suburbs {Santacruz (94 cm), Bhandup (81 cm), Dharavi (49), Vihar Lake (104 cm), Malabar Hill (7 cm), and Colaba (7 cm)} clearly demonstrated great spatial variability (Bohra et al. 2006). Also, the interplay of synoptic-scale weather systems with meso-scale coastal land-surface features, as well as inadequate rainfall size, extent, and intensity predictions by current weather-forecast models, may be the root causes of such rainfall vagaries. Furthermore, Nayak and Ghosh (2013) discovered that the high-speed wind flowing from the Arabian Sea brings surplus moisture which reduces away from the coastline was one of the important causes for the occurrence of this

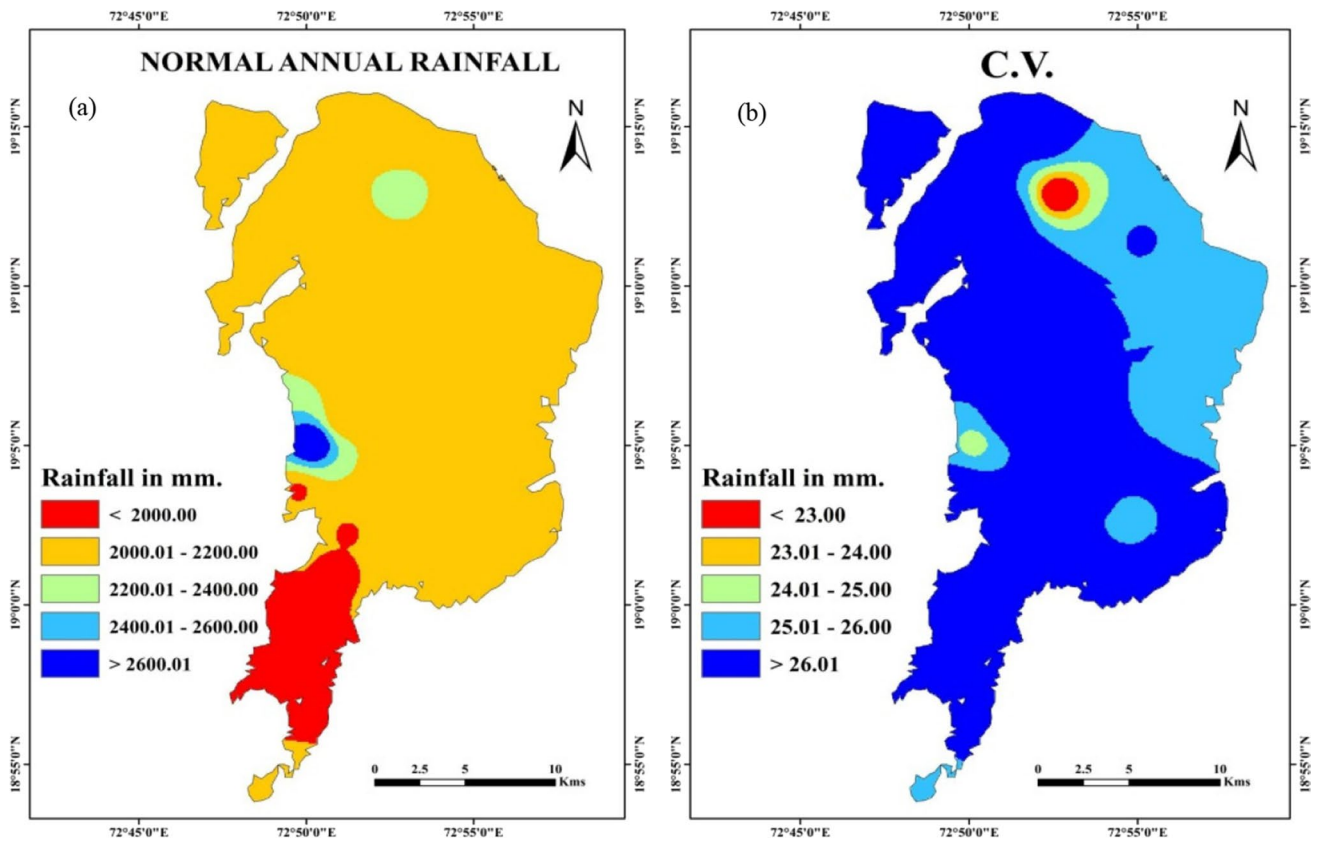


Fig. 2 Spatial distribution of **a** normal annual rainfall and **b** coefficient of variation over the study area (1985–2020)

differential behaviour of excessive rainfall on the west coast. Also, normal annual rainfall and temperature over Santacruz and Colaba are shown in Fig. 5. Normal annual rainfall over the study area follows the cyclic pattern of 5-year moving average over both the stations. Also, temperature shows rising trend over the time period (1985–2020). The detection of trends in the study area is computed by employing MK test and Sen's slope estimator. The test shows that rainfall is increasing at the rate of 22.081 mm/year at 95% confidence level (Table 4). Also, it is clearly seen from the slope value ($R=0.22$) calculated by using regression analysis that rainfall is increasing all over the study area. Furthermore, the value of C_k is 0.64 which also suggests that the rainfall over the study area as a whole has increased. The detection of trends in annual rainfall by using simple linear regression is shown in Fig. 6. Thus, from the above analysis, it was observed that though the rainfall over the study is highly erratic it has registered an increasing trend over the time period (1985–2020).

4.1.1 Extreme rainfall events

The events of annual maximum rainfall of different intensities over the study area are categorized using the scheme

of IMD mentioned in Table 3. In the present study, events only under two categories are considered that are very heavy and extremely heavy. A heavy rainfall event is defined when rainfall values range between 115.6 and 204.4 mm/day and extremely heavy for rainfall that exceeds 204.05 mm/day in accordance with the rainfall patterns over the study area. The intensities of both the categories of events over Santacruz and Colaba are shown in Fig. 7. From the bar graphs of the said station, it is clearly seen that the intensities of both the categories of events increased after 1994 in the case of Santacruz and in the case of Colaba after 2005. However, rainfall events of immensely high intensity are observed over Santacruz in 2005 having rainfall over 944 mm/day and in 2011 over Colaba having rainfall over 1058 mm/day. The events of 2005 are responsible for the flood havoc over Mumbai. The 2005 flood event caused extensive damage to Mumbai and surrounding areas. Mumbai Metropolitan Region (MMR) authorities reported 700 deaths, 244,110 houses destroyed or partially damaged, 97 collapsed school buildings, 5667 damaged electricity transformers, together with vehicular losses to national highways and transportation systems (52 broken local trains, 41,000 taxi cabs, 900 buses, 10,000 trucks). Trade and commerce suffered losses

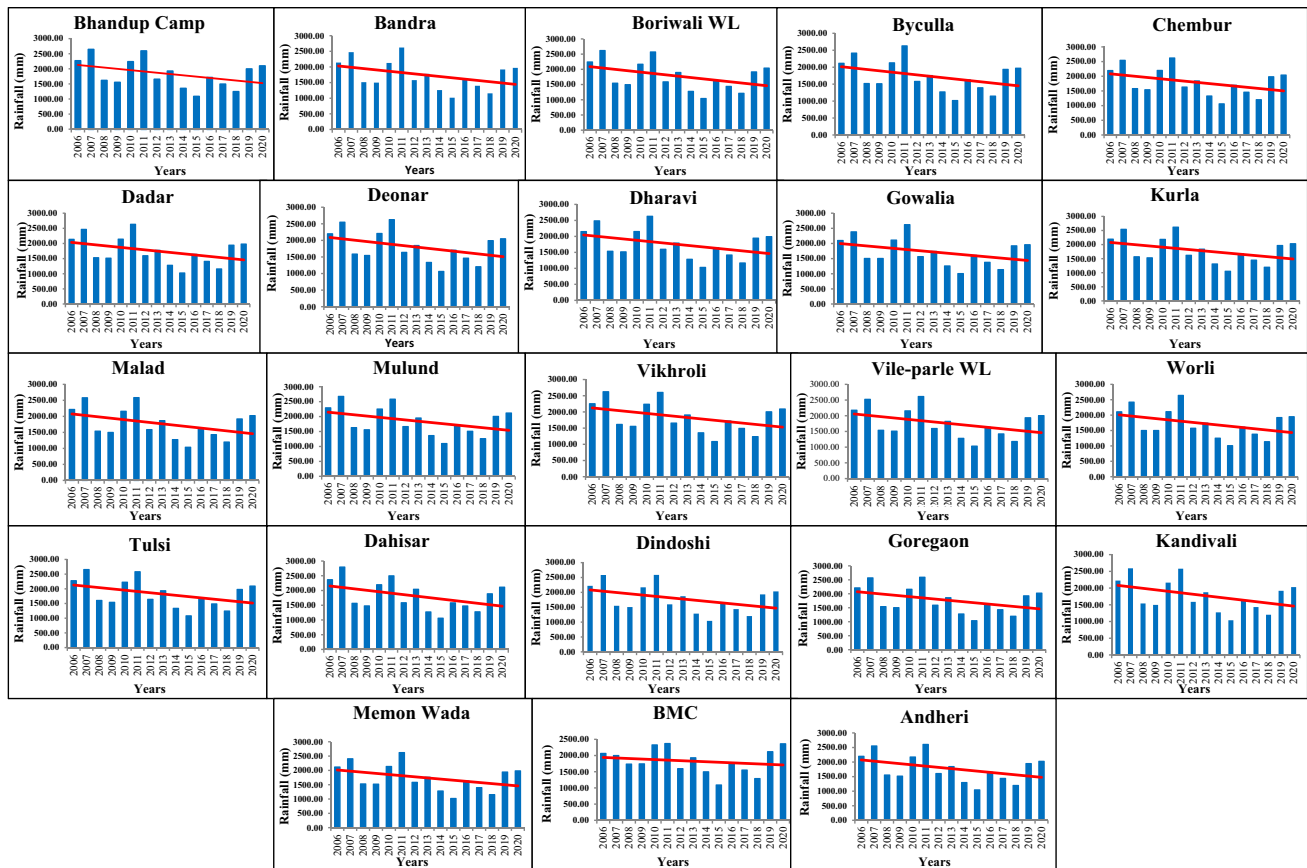


Fig. 3 Station-wise trends of average annual rainfall over the study area (2006–2020)

of 50 billion U.S. dollars (5000 cores) (Government of Maharashtra 2005; FFCMF 2006).

4.1.2 Change point detection

As it is difficult to determine which strategy is best for a given area and as each method has upsides and downsides, it is usually advised to use a variety of techniques to check the homogeneity and change points of data for a certain area. Therefore, four distinct tests, i.e. Pettitt's, SNH, Buishand range, and von Neumann ratio, have been used in this section to detect the abrupt change points in rainfall and temperature datasets. Table 5 illustrates the test statistics for these tests, as well as the null hypothesis acceptance or rejection in rainfall and temperature data series. Figures 8 and 9 depict the graphical representations of rainfall and temperature time series over Colaba and Santacruz with the most important positive (increasing) trends from 1985 to 2020 with their respective change points. The current variations in rainfall trend, major mechanisms, and inter-annual variability of Indian summer monsoon rainfall (ISMR) are explored in this study during the period 1985–2020. Rainfall data revealed a downward tendency from 1985 to 2005 (period

1), then a strong upward trend from 2006 to 2020 (period 2). The abrupt change point in rainfall time series is observed only over Santacruz station and the change point in the data series starts from 2005 whereas at the rest of the stations, no change point was detected in the data series. In the case of temperature dataset, change point detection is observed from 2001 onwards over Colaba and Santacruz (Fig. 9). The study reveals that two significant changes in the second period are likely to be the cause of ISMR's current upward trend. The first is increasing easterly wind anomalies from the equatorial Pacific, which are linked to recent cooling in the eastern Pacific; the second is enhanced cross-equatorial flow in the Indian Ocean, which is linked to increased land-sea thermal contrast. The main mode of ISMR variability and temperature increase during the second period, and the relationship with boundary forcing became stronger. After 2000, the first mode of ISMR became substantially linked to central and east Pacific SST anomalies (El-nino Southern Oscillation (ENSO)), but its relationship with key SST indices was weak before. Significant warming in the temperature record after the year 2001 was observed in the second phase, which is strongly linked to the Indian Ocean Dipole mode. During both periods, these modes represent the inter-annual

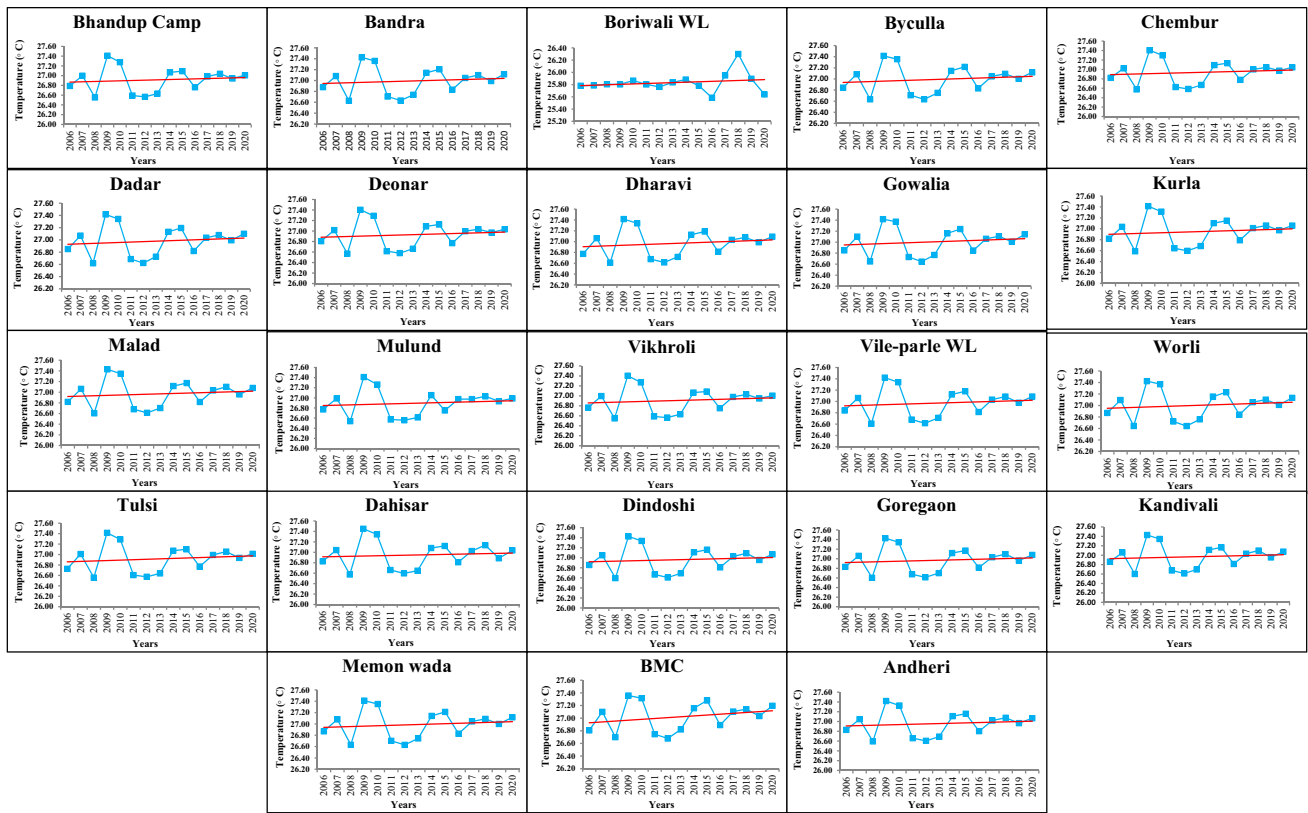


Fig. 4 Station-wise trends of average annual temperature over the study area (2006–2020)

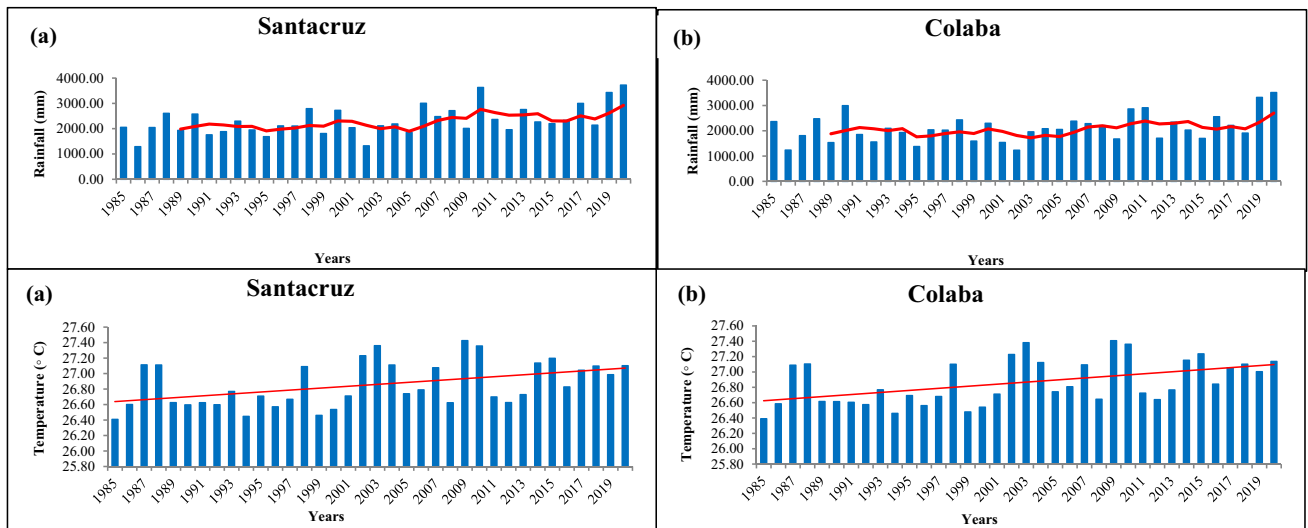


Fig. 5 Average annual rainfall and temperature over a Santacruz and c Colaba (1985–2020)

variability of ISMR, which increases significantly in the second. Another noteworthy difference between the two periods is that many of the severe monsoon events during period 1 were not related to ENSO, but many during period 2 were (Devika and Pillai 2020). The result of all the three tests

in the case of temperature time series shows change in the dataset from 2001 onwards. Both for rainfall and temperature, the study findings of change points from three distinct tests of homogeneity detection closely confirm each other at 99 and 95% significance levels. It is discovered that the von

Table 4 Mean (*M*), standard deviation (SD), coefficient of variation (CV), kurtosis (*C_K*), skewness (*C_S*), Mann–Kendall test (*Z*), Sen’s slope estimator (*Q*), and regression (*R*) of monthly, seasonal, and

annual rainfall over Mumbai based on the combined rainfall data of Colaba and Santacruz (1985–2020)

Time	<i>M</i> (mm)	S.D (mm)	CV (%)	<i>C_K</i>	<i>C_S</i>	% of annual	<i>Z</i>	<i>Q</i>	<i>R</i>
January	1.52	3.87	254.65	7.83	6.24	0.07	.14	00	0.03
February	7.34	42.15	574.51	35.97	5.12	0.33	1.24	.94	0.04
March	0.91	2.77	303.25	15.55	6.27	0.04	.49	.92	0.02
April	0.56	1.47	262.52	17.21	6.27	0.03	1.36	.016	0.09
May	22.80	62.12	272.39	12.79	2.94	1.03	1.37	.014	0.01
June	516.49	248.66	48.14	−0.23	0.27	23.38	.34	1.604	0.01
July	752.75	319.37	42.43	−0.32	0.03	34.08	2.90**	14.95**	0.22
August	487.98	229.95	47.12	0.24	0.59	22.09	.29	.896	0.00
September	324.30	216.23	66.68	1.89	1.10	14.68	1.08	4.62	0.07
October	80.64	85.45	105.96	2.70	1.57	3.65	.59	.331	0.00
November	8.26	15.15	183.43	6.63	4.57	0.37	2.11*	.018*	0.13
December	5.26	14.95	284.36	22.53	5.50	0.24	1.24	00	0.05
Winter (January–February)	8.86	21.34	481.97	35.32	5.73	0.40	1.23	00	0.05
Pre-monsoon (March–May)	24.28	20.95	258.89	12.19	4.73	1.10	1.59	.013	0.00
Monsoon (June–September)	2081.53	123.96	23.82	1.04	−0.77	94.24	2.60**	5.177*	0.23
Post-monsoon (October–December)	94.16	28.50	90.82	2.60	1.29	4.26	.75	.271	0.00
Annual	2208.82	44.38	24.11	0.64	−0.71	100	2.47*	22.081*	0.22

*95% confidence level, **99% confidence level

Fig. 6 Trends in average annual rainfall and temperature over the study area using regression analysis (1985–2020)

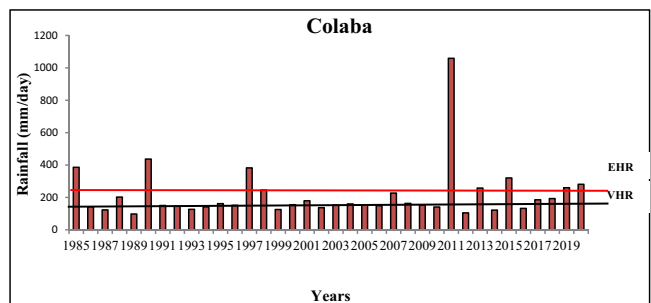
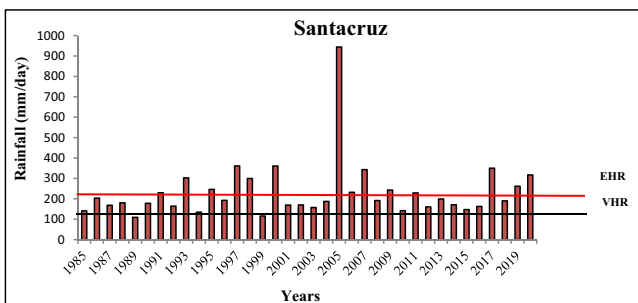
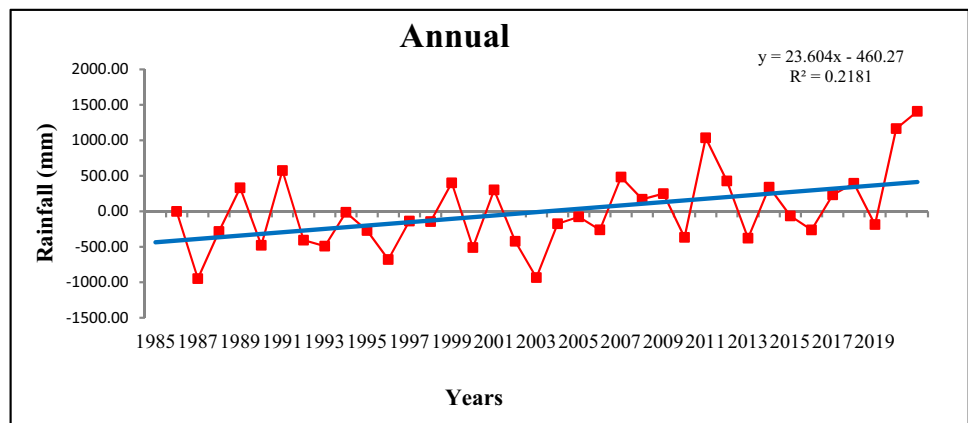


Fig. 7 Heavy and extreme heavy rainfall events over Santacruz and Colaba (1985–2020)

Table 5 Results of abrupt change point analysis for rainfall and temperature over Mumbai 1985–2020

District	Station	Pettitt's test				SNH test				Buishand's test				Von Neumann's test			
		Statistic (K)	P value	Shift	Year of shift	Statistic (T°)	P value	Shift	Year of shift	Statistic (Q)	P value	Shift	Year of shift	Statistic (N)	P value	Shift	Nature of shift
Mumbai City	Colaba	143	.183	No	–	12.308	.006	No	–	7.326	.06	No	–	1.655	.150	No	HO
	Santacruz	205	.008	Positive	2005	10.69	.015	No	–	9.646	.003	Positive	2005	1.612	.12	No	HO
Mumbai sub-urban	Colaba	241	00	Positive	2001	12.461	.003	Positive	2001	10.724	.002	Positive	2001	1.193	.007	Yes	CP
	Santacruz	222	.002	Positive	2001	11.342	.006	Positive	2001	10.231	.003	Positive	2001	1.252	.012	Yes	CP

HO homogenous, CP change point

Neumann ratio test findings cannot be evaluated because it provides results for both positive and negative change points.

4.2 Seasonal analysis

The seasonal description of different determinants is given in Table 4. For that, rainfall data of two stations (Colaba and Santacruz) are merged and analyses are performed. It is done because of the discontinuity (or later setup of rain gauge stations by MCGM after the flood event of 2005) of the dataset of remaining 23 stations. Average annual rainfall in the monsoon season is about 2081.53 mm having SD values ranging from 20.95 to 123.96 mm. The value of *R* (regression) is also high in the month of monsoon which shows that the rate of increase in rainfall is high. The graphical representation of rainfall by using linear regression is shown in Fig. 10. It shows that the rainfall in all seasons is increasing but the gradient or slope of change is high in monsoon season only. Furthermore, spatial distribution of seasonal rainfall all over the study area is shown in Fig. 11. It shows that in the winter season, rainfall is high over Santacruz station and low over the southern tip of Mumbai city, i.e. Colaba. The contrasting nature of ISMR is clearly seen in the rainfall distribution map of monsoon season, i.e. high rainfall over Colaba, Bandra, and Santacruz station and low over Mulund and Bhandup camp. A different trend in rainfall is observed in pre- and post-monsoon seasons. In post-monsoon season, rainfall all over the study area is high except over Colaba and Santacruz, i.e. areas of high rainfall in monsoon are the areas of low rainfall in post-monsoon season. An opposite trend is observed in pre-monsoon season. The values of CV are highest in the month.

of winter (481.97%) because winter season is not a rainfall season whereas CV in monsoon season is 23.82%. Thus, we can say that the study area lies in moderate variability zone. Interestingly, about 95% of total rainfall occurs in monsoon season and rest of the seasons only receives about 5% of total rainfall. The change in rainfall trends is calculated using MK statistic and the value of *Z* signifies the level of significant change in the data series. The *Z* statistic shows that rainfall shows an increasing trend only in monsoon season which is at the rate of 5.177 mm/year at 99% significance level (Table 4).

4.3 Monthly analysis

In this section also, only two stations (Colaba and Santacruz) are included in the analyses because of the discontinuity of the dataset. CV was calculated and reported in Table 4 to better understand the variability of mean monthly rainfall over the study area. (Standard deviation/mean) * 100 were used to determine the CV. CV during different months is depicted in this table. Rainfall seems to be highly variable

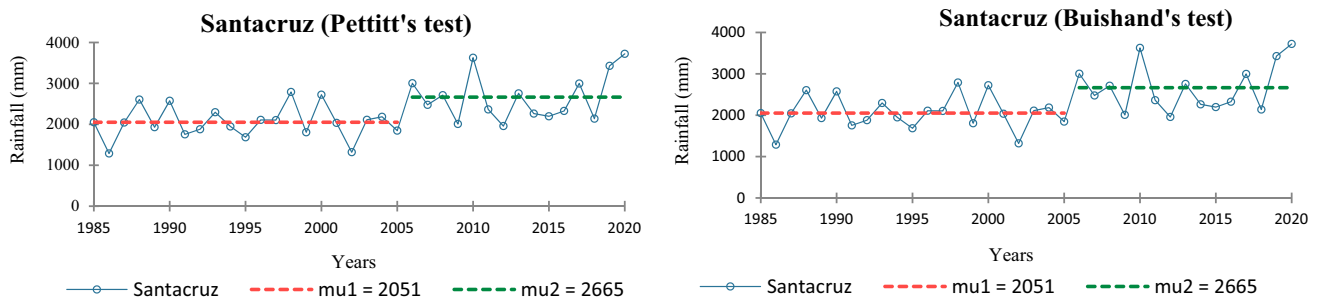


Fig. 8 Abrupt change point detection in rainfall time series data over Santacruz by using different tests (1985–2020)

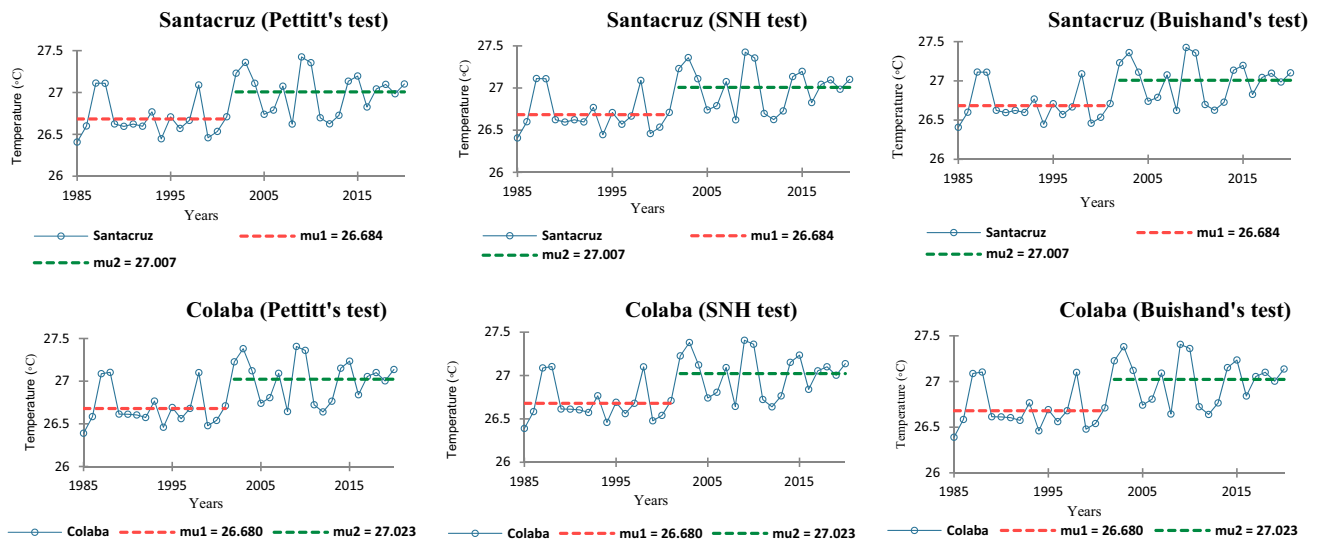


Fig. 9 Abrupt change point detection in temperature time series data over Santacruz and Colaba by using different tests (1985–2020)

over the entire study area, having CV values ranging from 42.43% in July to 574.5% (in February). This illustrates the complexities of rainfall patterns in the studied area. The average monthly rainfall ranges from 0.56 mm in January to 752.75 mm in July. Thus, it is clearly seen from the discussion that July is the month of heavy rainfall over the entire study area. Similarly, the value of CV is high in the active monsoon month of September which is 66.68%. The rainfall behaviour is highly erratic as we look at the SD value that ranges between 1.47 and 319.37 mm. Furthermore, it is clearly seen in the table that about 80% of annual rainfall has occurred only in 3 months, i.e. June, July, and August. The value of Z statistic or MK test signifies that change in rainfall was observed only in the months of July and November. It is increasing at the rate of 14.95 mm/year in July (at 99% confidence level) and 0.018 mm/year in November (at 95% confidence level). Furthermore, the spatial distribution pattern of monthly rainfall is shown in Fig. 12. It clearly shows that the distribution of monthly rainfall is furcating, as one moves from northeast to southwest.

5 Conclusion

A detailed assessment of hourly rainfall at 2 rain gauge stations spread through two districts of Maharashtra (Mumbai city and sub-urban), India, spanning for 36-year period between 1985 and 2020 was carried out. Distance matrix tool in ArcGIS is used to pick distinct stations. Many rainfall datasets have been accessible in recent years, but in this study, an hourly rainfall analysis across Greater Mumbai utilizing a dense network of 23 rain gauge stations from MCGM for the last 15 years (2006–2020) is also performed. The aspects examined are rainfall's climatological behaviour, its variability, and extreme events over Mumbai, as well as a detailed analysis of different severe event intensities. Using datasets for rainfall amounts, CV, maximum daily rainfall, rainfall intensity, abrupt change point detection in rainfall and temperature time series, monthly and seasonal climatology for each rain gauge station have been derived.

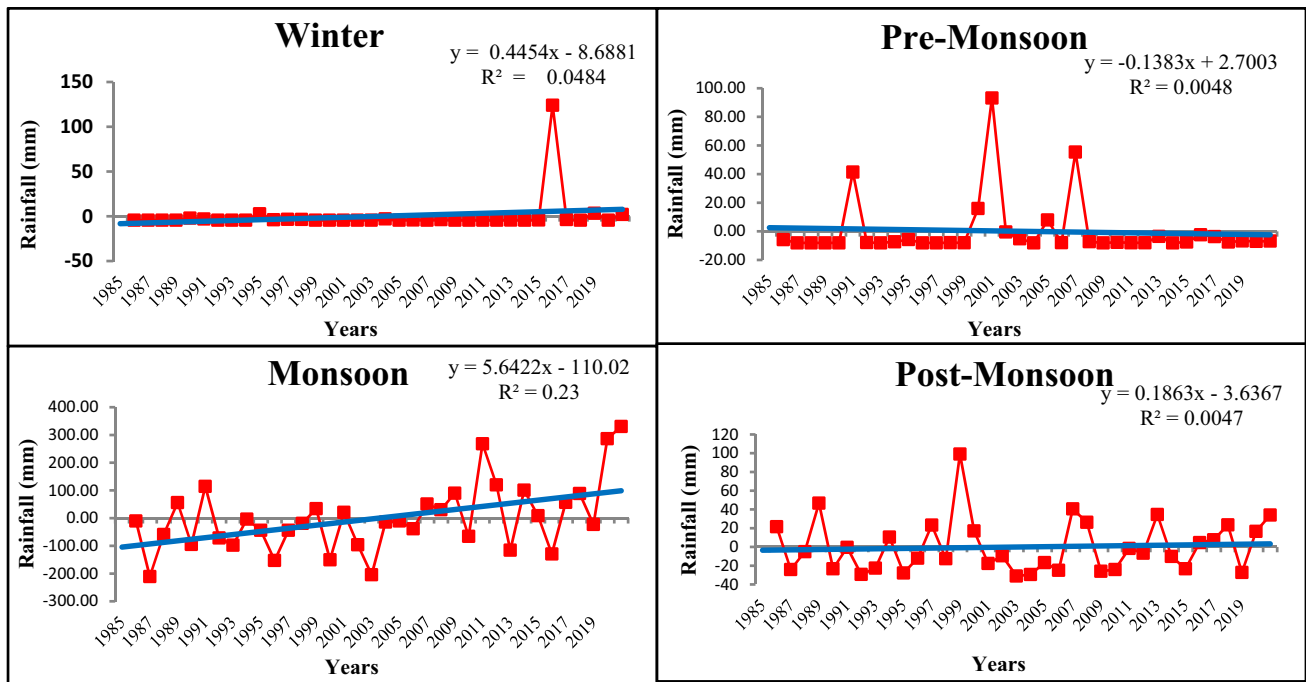


Fig. 10 Seasonal rainfall trend over the study area using regression analysis (1985–2020)

The spatial patterns of rainfall revealed that the rainfall is primarily concentrated near Colaba and Santacruz stations. Total rainfall over central Mumbai is high, and it falls across a vast area from June to September. The rainfall is high during the active monsoon months and is low during the onset and retreating phase of the monsoon. Rainfall distribution of annual rainfall over the study area shows more than 2600 mm over Santacruz and 2000–2400 mm in rest of the stations of the study area. This suggests that rainfall patterns are highly variable in terms of both geographical and temporal variability across the whole study area. Rainfall is steadily decreasing from central Mumbai to eastern Mumbai (areas near Mulund, Tulsī, BMC, Vikhroli, and other stations). The Arabian Sea branch of the monsoon influences the entire study region, which receives 2208.82 mm of rainfall. The spatial distribution of climatological rainfall suggests that the southern and western areas of Mumbai receive higher rainfall. The eastern and northern parts of Mumbai get less rain than rest of the city. The rainfall is highly variable across the entire study area, demonstrating the complexities of rainfall occurrence across Mumbai. The study area falls in the moderate variability zone. CV values in the study area decrease around Santacruz and BMC station, indicating high variability in rest of Mumbai. Its proportions drop from 27.91% in Dahisar to 21.25% in BMC. The results of abrupt change point detection indicate that rainfall has been increasing significantly after 2005 only over Santacruz station (in accordance with Pettitt's and Buis-hand test) whereas, in the case of temperature, the point of

change in data series is observed after 2001 over Colaba and Santacruz in all four tests. The rest of the stations show no significant changes in the time series data. Santacruz station has the highest number and intensity of extreme incidents, followed by Colaba. The rest of the stations, on the other hand, have not seen much rain in the study area. In comparison to July and August, extreme events are lower in June and September because June is the onset month, September is the withdrawal month, and July and August are the active monsoon months over the study area. Moreover, it is observed that rainfall has increased over Santacruz and Colaba during July and August. Both heavy and extremely heavy rainfall events have also increased in the study area. In the case of Santacruz, increase has been observed after 1994 while over Colaba it has been observed after 2005.

It is usually observed that the rains cripple the daily activities of people in Mumbai city hampering the industrial and tertiary services. The lifeline of Mumbai city, the local trains, their services are also affected with greater intensity during a wet spell. Increase in the heavy and extremely heavy events over Mumbai has thrown a greater challenge for the city administration. The work further calls upon demarcation of low-lying area with respect to their vulnerability of floods during heavy rains so as to identify areas for better management of flood waters, particularly during Monsoon season. Despite the fact that this work is limited to 15 years of data from 23 stations and 36 years of data from two stations from the recent time, it throws light on the spatial variation of rainfall over the area. As the length

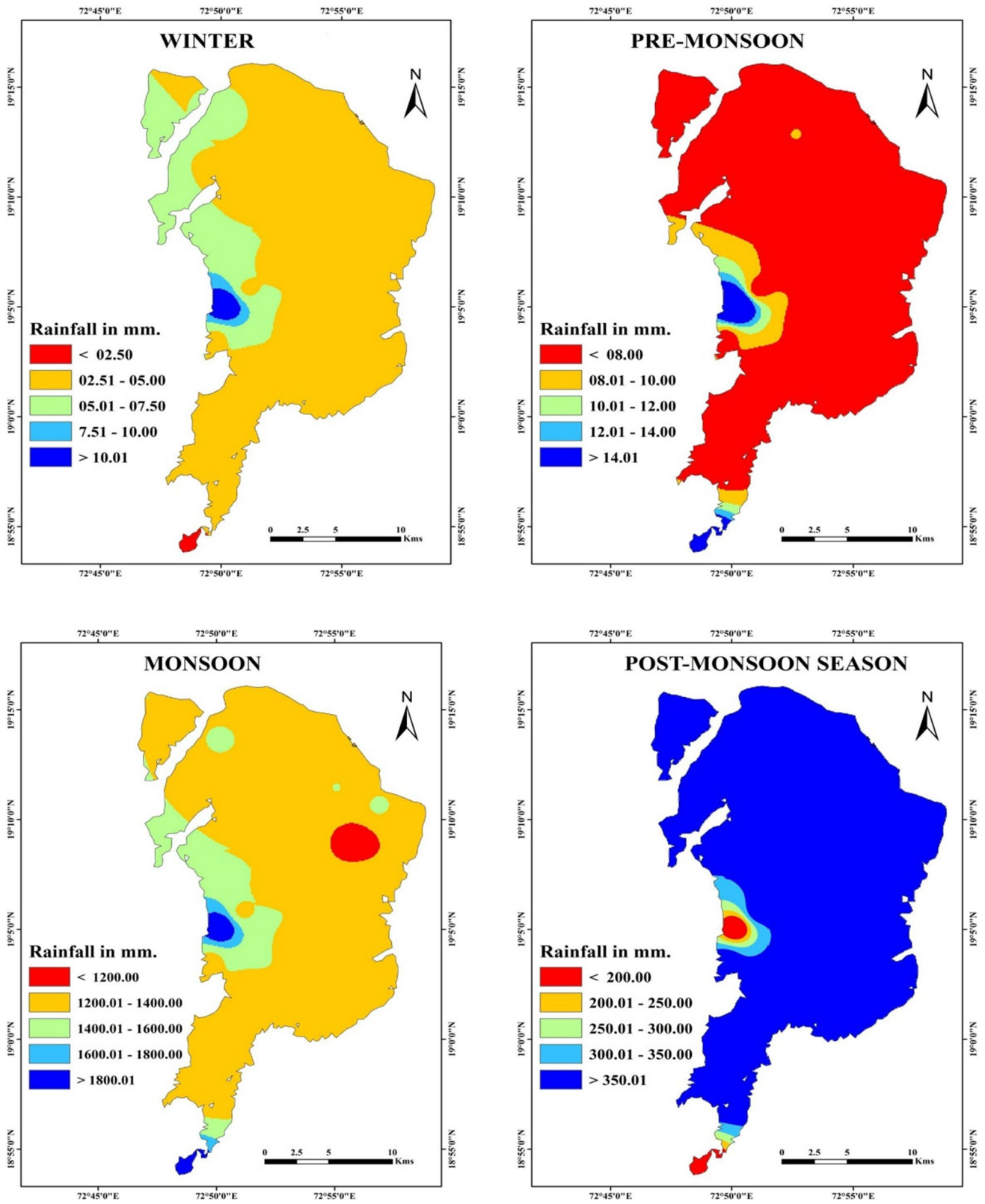


Fig. 11 Spatial distribution of seasonal rainfall over the study area (1985–2020)

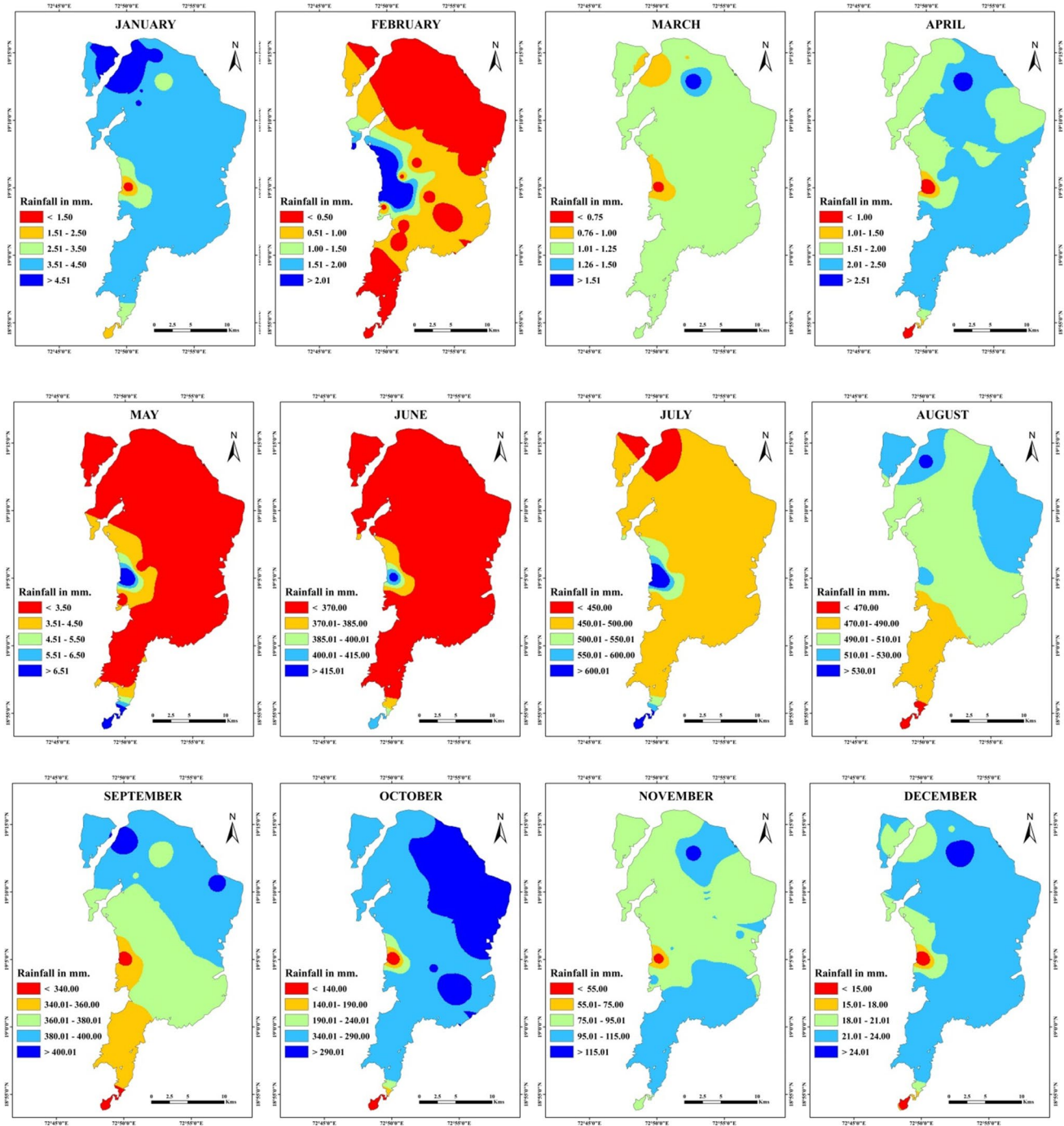


Fig. 12 Spatial distribution of monthly rainfall over the study area (1985–2020)

of datasets from these new stations will increase, more details of the rainfall climatology will be available to the administrators.

The findings of this study strongly imply that extreme weather events and variability of rainfall have an impact on the surrogate observations that are the subject of this investigation. Furthermore, considering that temperature trends have the greatest impact on rainfall trends, we should

anticipate that these trends will persist given the predictions of further increase in extreme rainfall events in the near future. The use of rainfall variability in accordance with scenarios of extreme events may currently be the best strategy for understanding the overall effects of climate change on the rainfall behaviour along the west coast of India because rainfall variability seems most strongly associated with decadal variability rather than long-term trends. Such a strategy

also means that “rainfall variability” and “extreme events” are likely to happen in the future at different locations, and MCGM authorities must take these possibilities into account when testing alternate management plans for Mumbai.

Author contribution R. Mann analyzed data, did literature review, and drafted the initial manuscript. A. Dhorde and S. Sharma provided research direction and assisted in writing and editing of the manuscript. A. Dhorde A. Gupta and S. Sharma took lead in the supervision, guided research direction, and assisted in the writing and editing of the manuscript. The listed authors have made a significant contribution to warrant their being part of authorship and have approved the work.

Data availability The data will be made available on demand.

Code availability Not applicable.

Declarations

Ethics approval Not applicable.

Consent to participate The authors express their consent to participate for research and review.

Consent for publication The authors express their consent for publication of research work.

Conflict of interest The authors declare no competing interests.

References

- Aguilar E, Peterson TC, Obando PR, Frutos R, Retana JA, Solera M, Soley J, García IG, Araujo RM, Santos AR, Valle VE, Brunet M, Aguilar L, Álvarez L, Bautista M, Castañón C, Herrera L, Ruano E, Sinay JJ, Mayorga R (2005) Changes in precipitation and temperature extremes in Central America and northern South America, 1961–2003. *J Geophys Res Atmos* 110(23):1–15. <https://doi.org/10.1029/2005JD006119>
- Ahmed K, Shahid S, Ismail T, Nawaz N, Wang XJ (2018) Absolute homogeneity assessment of precipitation time series in an arid region of Pakistan. *Atmósfera* 31:301–316. <https://doi.org/10.20937/atm.2018.31.03.06>
- Ahmed K, Nawaz N, Khan N, Rasheed B, Baloch A (2021) Inhomogeneity detection in the precipitation series: case of arid province of Pakistan. *Environ Develop and Sustain* 23:7176–7192. <https://doi.org/10.1007/s10668-020-00910-y>
- Alexander LV, Zhang X, Peterson TC, Caesar J, Gleason B, Klein Tank AMG, Haylock M, Collins D, Trewin B, Rahimzadeh F, Tagipour A, Rupa Kumar K, Revadekar J, Griffiths G, Vincent L, Stephenson DB, Burn J, Aguilar E, Brunet M, Vazquez-Aguirre JL (2006) Global observed changes in daily climate extremes of temperature and precipitation. *J Geophys Res Atmos* 111(5). <https://doi.org/10.1029/2005JD006290>
- Alexandersson HA (1986) A homogeneity test applied to precipitation data. *Int J Climatol* 6:661–675. <https://doi.org/10.1002/joc.3370060607>
- Amirabadizadeh M, Huang YF, Lee TS (2015) Recent trends in temperature and precipitation in the Langat River Basin, Malaysia. *Adv Meteorol* 2015:579437. <https://doi.org/10.1155/2015/579437>
- Asakereh H (2016) Trends in monthly precipitation over the north-west of Iran (NWI). *Theor Appl Climatol* 1–9. <https://doi.org/10.1007/s00704-016-1893-8>
- Ashrit RG, Rupa Kumar K, Krishna Kumar K (2001) ENSO-Monsoon relationship in a greenhouse warming scenario. *Geophys Res Lett* 28(9):1727–1730. <https://doi.org/10.1029/2000GL012489>
- Bari SH, Rahman MTU, Hoque MA, Hussain MM (2016) Analysis of seasonal and annual rainfall trends in the northern region of Bangladesh. *Atmos Res* 176–177:148–158. <https://doi.org/10.1016/j.atmosres.2016.02.008>
- Bohra AK, Basu S, Rajagopal EN, Iyengar GR, Gupta MD, Ashrit R, Athiyaman B (2006) Heavy rainfall episode over Mumbai on 26 July 2005: assessment of NWP guidance. *Curr Sci* 90(9):1188–1194 (<https://core.ac.uk/download/pdf/151497029.pdf>). Accessed 16 Nov 2022
- Buishand TA (1982) Some methods for testing the homogeneity of rainfall records. *J Hydro* 58:11–27. [https://doi.org/10.1016/0022-1694\(82\)90066-X](https://doi.org/10.1016/0022-1694(82)90066-X)
- Bussi eres N, Hogg W (1989) The objective analysis of daily rainfall by distance weighting schemes on a mesoscale grid. *Atmos Ocean* 27(3):521–541. <https://doi.org/10.1080/07055900.1989.9649350>
- Buytaert W, Celleri R, Willems P, De Bievre B, Wyseure G (2006) Spatial and temporal rainfall variability in mountainous areas: a case study from the south Ecuadorian Andes. *J Hydrol* 329(3):413–421. <https://doi.org/10.1016/j.jhydrol.2006.02.031>
- Carrera-Hernandez JJ, Gaskin SJ (2007) Spatio-temporal analysis of daily precipitation and temperature in the Basin of Mexico. *J Hydrol* 336(3):231–249. <https://doi.org/10.1016/j.jhydrol.2006.12.021>
- Census of India (2011) Primary census abstract, census of India, Govt of India. <https://censusindia.gov.in/census.website/data/census-tables>. Accessed 12 June 2022
- Chandniha SK, Meshram SG, Adamowski JF, Meshram C (2016) Trend analysis of precipitation in Jharkhand State, India. *Theor Appl Climatol* 130:1–14. <https://doi.org/10.1007/s00704-016-1875-x>
- Chang HI, Kumar A, Niyogi D, Mohanty UC, Chen F, Dudhia J (2009) The role of land surface processes on the mesoscale simulation of the July 26, 2005 heavy rain event over Mumbai, India; *Global Planet Change* 67(1):87–103. <https://doi.org/10.1016/j.gloplacha.2008.12.005>
- Dahdouh-Guebas F, Jayatissa LP, Di Nitto D, Bosire JO, Lo Seen D, Koedam N (2005) How effective were mangroves as a defence against the recent tsunami? *Curr Biol* 15(12):R443–R447. <https://doi.org/10.1016/j.cub.2005.06.008>
- Dash SK, Kulkarni MA, Mohanty UC, Prasad K (2009) Changes in the characteristics of rain events in India. *J Geophys Res Atmos* 114(D10):D10109. <https://doi.org/10.1029/2008JD010572>
- Devika MV, Pillai PA (2020) Recent changes in the trend, prominent modes, and the inter-annual variability of Indian summer monsoon rainfall centered on the early twenty-first century. *Theoret Appl Climatol* 139(1–2):815–824. <https://doi.org/10.1007/s00704-019-03011-7>
- Dhorde A, Dhorde A, Gadgil S (2009) Long-term temperature trends at four largest cities of India during the twentieth century. *J Ind Geophys Union* 13(2):85–97 (<https://www.researchgate.net/publication/264876137>). Accessed 8 July 2022
- Easterling DR, Horton B, Jones PD, Peterson CT, Karl TR, Parker DE, Salinger MJ, Razuvayev V, Plummer N, Jamason P, Folland CK (1997) Maximum and minimum temperature trends for the globe. *Science* 277:364–367. <https://doi.org/10.1126/science.277.5324.364>
- Emery KO, Aubrey DG (1991) Sea levels, land levels, and tide gauges. Berlin, Heidelberg, New York. Pub. Springer-Verlag. <https://openlibrary.org/search?q=Sea+Levels%2C+Land+Levels%2C+and+Tide+Gauges&mode=everything>

- Farajzadeh J, Fakheri Fard A, Lotfi S (2014) Modeling of monthly rainfall and runoff of Urmia lake basin using “feed-forward neural network” and “time series analysis” model. *Water Resour Ind* 7–8:38–48. <https://doi.org/10.1016/j.wri.2014.10.003>
- Fathian F, Aliyari H, Kahya E, Dehghan Z (2016) Temporal trends in precipitation using spatial techniques in GIS over Urmia Lake Basin, Iran. *Int J Hydrol Sci Technol* 6(1):62–81. <https://doi.org/10.1504/IJHST.2016.073883PDF>
- FFC (Fact Finding Committee) Report on Mumbai Floods (2006) Maharashtra State Government committee Report, 1–359. <https://pdfslide.net/documents/fact-finding-committee-on-mumbai-floods-vol1.html?page=5>
- Folland CK, Karl TR, Christy JR, Clarke RA, Grouza GV, Jouzel J, Mann ME, Oerlemans J, Salinger MJ, Wang SW (2001) Observed climate variability and change, in *Climate Change 2001: The Scientific Basis—Contribution of Working Group I to the Third Assessment Report of the Intergovernmental Panel on Climatic Change*, edited by J. T. Houghton et al. pp. 85–97, Cambridge Univ. Press, New York. <https://www.ipcc.ch/site/assets/uploads/2018/03/TAR-02.pdf>. Accessed 4 June 2022
- Frich P, Alexander LV, Della-Marta P, Gleason B, Haylock M, Klein Tank AMG, Peterson T (2002) Observed coherent changes in climatic extremes during the 2nd half of the 20th century. *Clim Res* 19:193–212. <https://doi.org/10.3354/cr019193>
- Gadgil A (1986) Annual and weekly analysis of rainfall and temperature for Pune: a multiple time series approach. *Inst Indian Geographers* 8(1):14–20 (https://www.researchgate.net/publication/321016535_SpatioTemporal_Analysis_of_Rainfall_Distribution_and_Variability). Accessed 19 June 2022
- Geodetic and Research Branch Report (2006) In: Anon. (eds) Indian tide table part I. Indian and selected foreign ports: government of India. Surveyor General of India, Dehradun, India. https://surveyofindia.gov.in/files/GRB_RTI_DATA.pdf. Accessed 23 June 2022
- Geodetic and Research Branch Report (2013) In: Anonymous. (eds) Indian tide tables part I (p. 238). Government of India, Surveyor General of India, Dehradun, India. https://www.surveyofindia.gov.in/files/GRB_RTI_DATA.pdf. Accessed 23 June 2022
- Goswami BN, Venugopal V, Sengupta D, Madhusoodanan MS, Xavier PK (2006) Increasing trend of extreme rain events over India in a warming environment. *Science* 314(5804):1442–1445. <https://doi.org/10.1126/science.1132027>
- Government of Maharashtra (2005) Maharashtra state disaster management plan. State disaster management authority Mantralaya, Mumbai. https://rfd.maharashtra.gov.in/sites/default/files/DM%20Plan%20final_State.pdf. Accessed 28 June 2022
- Guerreiro SB, Kilsby CG, Serinaldi F (2014) Analysis of time variation of rainfall in transnational basins in Iberia: Abrupt changes or trends? *Int J Climatol* 34:114–133 (<https://rmets.onlinelibrary.wiley.com/journal/10970088>)
- Gunnell Y (1997) Relief and climate in South Asia: the influence of the Western Ghats on the current climate pattern of peninsular India. *Int J Climatol* 17:1169–1182. [https://doi.org/10.1002/\(SICI\)1097-0088\(199709\)17:11%3C1169::AID-JOC189%3E3.0.CO;2-W](https://doi.org/10.1002/(SICI)1097-0088(199709)17:11%3C1169::AID-JOC189%3E3.0.CO;2-W)
- Hallegatte S, Green C, Nicholls RJ, Corfee-Morlot J (2013) Future flood losses in major coastal cities. *Nat Clim Change* 3(9):802–806. <https://doi.org/10.1038/NCLIMATE1979>
- Hamlet AF, Mote PW, Clark MP, Lettenmaier DP (2005) Effects of temperature and precipitation variability on snowpack trends in the Western United States. *J Climate* 18(21):4545–4561. <https://doi.org/10.1175/JCLI3538.1>
- Hansen J, Ruedy R, Sato M, Imhoff M, Lawrence W, Easterling D, Peterson T, Karl T (2001) A closer look at United States and global surface temperature change. *J Geophys Res* 106(23):947–963. <https://doi.org/10.1029/2001JD000354>
- Hanson S, Nicholls R, Ranger N, Hallegatte S, Corfee-Morlot J, Herweijer C, Chateau J (2011) A global ranking of port cities with high exposure to climate extremes. *Clim Change* 104:89–111. <https://doi.org/10.1007/s10584-010-9977-4>
- Hare W (2003) Assessment of knowledge on impacts of climate change, contribution to the specification of art, 2 of the UNFCCC: Impacts on Ecosystems, Food Production, Water and Socio-economic Systems, WBGU. https://www.researchgate.net/publication/242460387_Assessment_of_Knowledge_on_Impacts_of_Climate_Change_Contribution_to_the_Specification_of_Art_2_of_the_UNFCCC_Impacts_on_Ecosystems_Food_Production_Water_and_Socio-economic_Systems. Accessed 5 June 2022
- Haylock M R, et al. (2006) Trends in total and extreme South American rainfall 1960–2000 and links with sea surface temperature. *J Climate* 18(23). <https://doi.org/10.1175/JCLI3589.1>
- Haylock M, Nicholls N (2000) Trends in extreme rainfall indices for an updated high quality data set for Australia, 1910–1998. *Int J Climatol* 20:1533–1541. [https://doi.org/10.1002/1097-0088\(200011\)20:13%3C1533::AID-JOC586%3E3.0.CO;2-](https://doi.org/10.1002/1097-0088(200011)20:13%3C1533::AID-JOC586%3E3.0.CO;2-)
- IMD (2007) Annual climate summary. IMD, Government of India. 1–135. <https://www.tropmet.res.in/~kolli/MOL/Monsoon/year2007/Monsoon-2007.pdf>
- IMD (2021) Standard operation procedure- weather forecasting and warning services. Ministry of Earth Sciences, Government of India. 1–331. https://mausam.imd.gov.in/imd_latest/contents/pdf/forecasting_sop.pdf
- Jaiswal RK, Lohani AK, Tiwari HL (2015) Statistical analysis for change detection and trend assessment in climatological parameters. *Environ Processes* 2:729–749. <https://doi.org/10.1007/s40710-015-0105-3>
- Jenamani RK, Bhan SC, Kalsi SR (2006) Observational/forecasting aspects of the meteorological event that caused a record highest rainfall in Mumbai. *Curr Sci* 90(10):1344–1362 (https://www.researchgate.net/publication/257343190_Observational_forecasting_aspects_of_the_meteorological_event_that_caused_a_record_highest_rainfall_in_Mumbai). Accessed 18 June 2022
- Jin Q, Wang C (2017) A revival of Indian summer monsoon rainfall since 2002. *Nat Clim Chang* 7:587–594. <https://doi.org/10.1038/nclimate3348>
- Jitendra S, Sheeba S, Subhankar K, Subimal G, Zope PE, Eldho TI (2017) Spatio-temporal analysis of sub-hourly rainfall over Mumbai, India: is statistical forecasting futile? *J Earth Syst Sci* 126:38. <https://doi.org/10.1007/s12040-017-0817-z>
- Jones PD, Moberg A (2003) Hemispheric and large-scale surface air temperature variations: an extensive revision and an update to 2001. *J Climate* 16:206–223. [https://doi.org/10.1175/1520-0442\(2003\)016%3C0206:HALSSA%3E2.0.CO;2](https://doi.org/10.1175/1520-0442(2003)016%3C0206:HALSSA%3E2.0.CO;2)
- Kendall MG (1948) Rank correlation methods. Griffin, London. <https://doi.org/10.2307/2333282>
- Khalili K, Tahoudi M, Mirabbasi R, Ahmadi F (2015) Investigation of spatial and temporal variability of precipitation in Iran over the last half century. *Stoch Env Res Risk A*:1–17. <https://doi.org/10.1007/s00477-015-1095-4>
- Klein Tank AMG et al (2006) Changes in daily temperature and precipitation extremes in central and south Asia. *J Geophys Res* 111(D16):1–18. <https://doi.org/10.1029/2005JD006316>
- Klein Tank AMG, Konnen GP (2003) Trends indices of daily temperature and precipitation extremes in Europe, 1946–99. *J Climate* 16:3665–3680. [https://doi.org/10.1175/1520-0442\(2003\)016%3C3665:TIIODT%3E2.0.CO;2](https://doi.org/10.1175/1520-0442(2003)016%3C3665:TIIODT%3E2.0.CO;2)
- Korade MS, Dhorde AG (2016) Trends in surface temperature variability over Mumbai and Ratnagiri cities of coastal Maharashtra.

- India. *Mausam* 67(2):455–462. <https://doi.org/10.54302/mausam.v67i2.1352>
- Kothawale DR, Revadekar JV, Kumar KR (2010) Recent trends in pre-monsoon daily temperature extremes over India. *J Earth Sys Science* 119(1):51–65. <https://doi.org/10.1007/s12040-010-0008-7>
- Kripalani RH, Kulkarni A, Sabade SS, Khandekar ML (2003) Indian monsoon variability in a global warming scenario. *Nat Hazards* 29(2):189–206. <https://doi.org/10.1023/A:1023695326825>
- Krishnan R, Sabin TP, Ayantika DC, Kitoh A, Sugi M, Murakami H, Turner AG, Slingo JM, Rajendran K (2013) Will the South Asian monsoon overturning circulation stabilize any further? *Clim Dyn* 40(1–2):187–211. <https://doi.org/10.1007/s00382-012-1317-0>
- Kulkarni BS, Reddy DD (1994) The cluster analysis approach for classification of Andhra Pradesh on the basis of rainfall. *Mausam* 45(4):325–332. <https://doi.org/10.54302/mausam.v45i4.2505>
- Kumar KK, Kamala K, Rajagopalan B, Hoerling MP, Eischeid JK, Patwardhan SK, Srinivasan G, Goswami BN, Nemani R (2011) The once and future pulse of Indian monsoonal climate. *Clim Dyn* 36(11–12):2159–2170 (<https://www.yumpu.com/en/document/read/36344756/the-once-and-future-pulse-of-indian-monsoonal-climate>)
- Lal M, Meehl GA, Arblaster JM (2000) Simulation of Indian summer monsoon rainfall and its intra-seasonal variability in the NCAR climate system model. *Reg Environ Change* 1(3–4):163–179. <https://doi.org/10.1007/s101130000017>
- Lei M, Niyogi D, Kishitawal C, Pielke RA Sr, Beltrán-Przekurat A, Nobis TE, Vaidya SS (2008) Effect of explicit urban land surface representation on the simulation of the 26 July 2005 heavy rain event over Mumbai, India. *Atmos Chem Phys* 8(20):5975–5995 (<https://hal.archives-ouvertes.fr/hal-00304159/document>)
- Liuzzo L, Bono E, Sammartano V, Freni G (2015) Analysis of spatial and temporal rainfall trends in Sicily during the 1921–2012 period. *Theor Appl Climatol* 126(1):113–129. <https://doi.org/10.1007/s00704-015-1561-4>
- Lokanadham B, Gupta K, Nikam V (2009) Characterization of spatial and temporal distribution of monsoon rainfall over Mumbai. *J Hydraul Eng* 15(2):69–80. <https://doi.org/10.1080/09715010.2009.10514941>
- Mann HB (1945) Nonparametric tests against trend. *Econometrica*. <https://doi.org/10.2307/1907187>
- Manton MJ et al. (2001) Trends in extreme daily rainfall and temperature in southeast Asia and the South Pacific: 1916–1998 *Int J Climatol* 21:269–284. <https://doi.org/10.1002/joc.610>
- Markonis Y, Batelis SC, Dimakos Y, Moschou E, Koutsoyianis D (2016) Temporal and spatial variability of rainfall over Greece. *Theor Appl Climatol* 1–16. <https://doi.org/10.1007/s00704-016-1878-7>
- May W (2002) Simulated changes of the Indian summer monsoon under enhanced greenhouse gas conditions in a global time-slice experiment. *Geophys Res Lett* 29(7):22–31. <https://doi.org/10.1029/2001GL013808>
- May W (2004) Simulation of the variability and extremes of daily rainfall during the Indian summer monsoon for present and future times in a global time-slice experiment. *Clim Dyn* 22(2–3):183–204. <https://doi.org/10.1007/s00382-003-0373-x>
- May W (2011) The sensitivity of the Indian summer monsoon to a global warming of 2°C with respect to pre-industrial times. *Clim Dyn* 37(9–10):1843–1868. <https://doi.org/10.1007/S00382-010-0942-8>
- MCGM (2007) Greater Mumbai Disaster management action plan. Volume 1. <https://dm.mcg.gov.in/assets/pdf/Disaster%20Management%20Plan-%20City.pdf>. Accessed 16 June 2022
- McGranahan G, Balk D, Anderson B (2007) The rising tide: assessing the risks of climate change and human settlements in low elevation coastal zones. *Environ Urban* 19:17–37. <https://doi.org/10.1177/0956247807076960>
- Mondal A, Khare D, Kundu S (2015) Spatial and temporal analysis of rainfall and temperature trend of India. *Theor Appl Climatol* 122(1–2):143–158. <https://doi.org/10.1007/s00704-014-1283-z>
- Mondal A, Lakshmi V, Hashemi H (2018) Intercomparison of trend analysis of multisatellite monthly precipitation products and gauge measurements for river basins of India. *J Hydrol* 565:779–790. <https://doi.org/10.1016/j.jhydrol.2018.08.083>
- Naidu CV, Rao BRS, Rao DVB (1999) Climatic trends and periodicities of annual rainfall over India. *Meteorol Appl* 6(4):395–404. <https://doi.org/10.1017/S1350482799001358>
- Narkhedkar SG, Kumar Mitra A, Sinha SK, Mitra AK (2006) Barnes objective analysis scheme of daily rainfall over Maharashtra (India) on a mesoscale grid evaluation of satellite-derived precipitation. *Atmosfera* 19(2). <https://www.researchgate.net/publication/262622863>. Accessed 12 June 2022
- Nayak MA, Ghosh S (2013) Prediction of extreme rainfall event using weather pattern recognition and support vector machine classifier. *Theor Appl Climatol* 114(3–4):583–603
- Nema MK, Khare D, Adamowski J, Chandniha SK (2018) Spatio-temporal analysis of rainfall trends in Chhattisgarh State, Central India over the last 115 years. *J Water Land Dev* 36(1):117–128. <https://doi.org/10.2478/jwld-2018-0012>
- New M, Todd M, Hulme M, Jones P (2001) Precipitation measurements and trends in the twentieth century. *Int J Climatol* 21(15):1889–1922. <https://doi.org/10.1002/joc.680>
- Nicholls RJ, Hanson S, Herweijer C, Patmore N, Hallegatte S, Corfee-Morlot J, Château J, Muir-Wood R. (2008) Ranking port cities with high exposure and vulnerability to climate extremes: exposure estimates. OECD Environment Working Papers, No. 1, OECD Publishing, Paris. <https://doi.org/10.1787/011766488208>
- Nikam V, Gupta K (2013) SVM-based model for short-term rainfall forecasts at a local scale in the Mumbai urban area, India. *J Hydrol Eng* 19(5):1048–1052 (<https://ascelibrary.org/doi/epdf/10.1061/28ASCE/29HE.1943-5584.0000875>)
- Pacione M (2006) City profile—Mumbai. *Cities* 23(3):229–238. <https://doi.org/10.1016/2Fj.cities.2005.11.003>
- Pal I, Al-Tabbaa A (2010) Long-term changes and variability of monthly extreme temperatures in India. *Theor Appl Climatol* 100(1):45–56. <https://doi.org/10.1007/s00704-009-0167-0>
- Pal L, Ojha CSP, Chandniha SK, Kumar A (2019) Regional scale analysis of trends in rainfall using nonparametric methods and wavelet transforms over a semi-arid region in India. *Int J Climatol* 39(5):2737–2764. <https://doi.org/10.1002/joc.5985>
- Parthasarathy B, Kumar KR, Munot AA (1993) Homogeneous Indian monsoon rainfall variability and prediction. *Proc Indian Acad Sci Earth Planet Sci* 102(1):121–155 (<https://www.ias.ac.in/article/fulltext/jess/102/01/0121-0155>)
- Patwardhan SK, Asnani GC (2000) Meso-scale distribution of summer monsoon rainfall near the Western Ghats (INDIA). *Int J Climatol* 20(5):575–581. [https://doi.org/10.1002/\(SICI\)1097-0088\(200004\)20:5%3c575::AID-JOC509%3e3.0.CO;2-6](https://doi.org/10.1002/(SICI)1097-0088(200004)20:5%3c575::AID-JOC509%3e3.0.CO;2-6)
- Peterson TC et al (2002) Recent changes in climate extremes in the Caribbean region. *J Geophys Res* 107(D21):4601. <https://doi.org/10.1029/2002JD002251>
- Peterson TC, Vose RS (1997) An overview of the Global Historical Climatology Network temperature data base. *Bull Am Meteorol Soc* 78:2837–2849. [https://doi.org/10.1175/1520-0477\(1997\)078/3C2837:A00TGH/3E2.0.CO;2](https://doi.org/10.1175/1520-0477(1997)078/3C2837:A00TGH/3E2.0.CO;2)
- Pettitt AN (1979) A non-parametric approach to the change point problem. *J Appl Statist* 28(2):126–135. <https://doi.org/10.2307/2346729>
- Pillai PA, Nair RC, Vidhya CV (2019) Recent changes in the prominent modes of Indian Ocean Dipole in response to the tropical Pacific Ocean SST patterns. *Theor Appl Climatol* <https://drs.nio.org/drs/handle/2264/8185?show=full>. Accessed 16 June 2022

- Prabhakar AK, Singh KK, Lohani AK, Chandniha SK (2017) Long term rainfall variability assessment using modified Mann- Kendall test over Champua watershed, Odisha. *J Agrometeorol* 17(2):288–289. <https://doi.org/10.54386/jam.v19i3.676>
- Ramachandran G, Banerjee AK (1983) The sub-divisional rainfall distribution across the Western Ghats during the southwest monsoon season. *Mausam* 34(2):179–184. <https://doi.org/10.54302/mausam.v34i2.2390>
- Ramesh Kumar MR, Krishnan R, Sankar S, Unnikrishnan AS, Pai DS (2009) Increasing trend of “break-monsoon” conditions over India—role of ocean – atmosphere processes in the Indian Ocean. *Geosci Remote Sens Lett IEEE* 6(2):332–336. <https://doi.org/10.1016/j.wace.2013.07.006>
- Rana A, Uvo C, Bengtsson L, Parth Sarthi P (2012) Trend analysis for rainfall in Delhi and Mumbai. *India Clim Dyn* 38(1):45–56. <https://doi.org/10.1007/s00382-011-1083-4>
- Ranger N, Hallegatte S, Bhattacharya S, Bachu M, Priya S, Dhore K, Rafique F, Mathur P, Naville N, Henriot F, Herweijer C, Pohit S, Morlot JC (2011) An assessment of the potential impact of climate change on flood risk in Mumbai. *Clim Change* 104(1):139–167. <https://doi.org/10.1007/s10584-010-9979-2>
- Ratna SB (2012) Summer monsoon rainfall variability over Maharashtra. *India Pure Appl Geophysics* 169(1–2):259–273. <https://doi.org/10.1007/s00024-011-0276-4>
- Roth M (2000) Review of atmospheric turbulence over cities. *Quart J Roy Meteorol Soc* 126(564):941–990. <https://doi.org/10.1002/qj.49712656409>
- Roy S, Balling RC (2004) Trends in extreme daily precipitation indices in India. *Int J Climatol* 24(4):457–466. <https://doi.org/10.1002/joc.995>
- Rupakumar K, Sahai AK, Kumar KK, Patwardhan SK, Mishra PK, Revadekar JV, Kamala K, Pant GB (2006) High-resolution climate change scenarios for India for the 21st century. *Curr Sci* 90:334–345 (https://www.researchgate.net/publication/255613749_Highresolution_climate_change_scenarios_for_India_for_the_21st_century)
- Rusticucci M, Barrucand M (2004) Observed trends and changes in temperature extremes over Argentina. *J Clim* 17(20):4099–4107. [https://doi.org/10.1175/1520-0442\(2004\)017%3c4099:OTACIT%3e2.0.CO](https://doi.org/10.1175/1520-0442(2004)017%3c4099:OTACIT%3e2.0.CO)
- Sabade SS, Kulkarni A, Kripalani RH (2011) Projected changes in South Asian summer monsoon by multi-model global warming experiments. *Theor Appl Climatol* 103(3–4):543–565. <https://doi.org/10.1007/s00704-010-0296-5>
- Sabzevari AA, Zarenistanak M, Tabari H, Moghimi S (2015) Evaluation of precipitation and river discharge variations over southwestern Iran during recent decades. *J Earth Syst Sci* 124(2):335–352 (<https://www.ias.ac.in/article/fulltext/jess/124/02/0335-0352>)
- Sarker RP (1966) A dynamical model of orographic rainfall. *Monthly Weath Review* 94(9):555–572. [https://doi.org/10.1175/1520-0493\(1966\)94%3C555%3EADYNAMICAL%20MODEL%20OF%20OROGRAPHIC%20RAINFALL.pdf](https://doi.org/10.1175/1520-0493(1966)94%3C555%3EADYNAMICAL%20MODEL%20OF%20OROGRAPHIC%20RAINFALL.pdf)
- Semenov VS, Bengtsson LB (2002) Secular trends in daily precipitation characteristics: greenhouse gas simulation with a coupled AOGCM. *Clim Dyn* 19(2):123–140. <https://doi.org/10.1007/s00382-001-0218-4>
- Sen PK (1968) Estimates of the regression coefficient based on Kendall’s tau. *J Am Stat Assoc* 63(324):1379–1389. <https://doi.org/10.1080/01621459.1968.10480934>
- Sen S, Vittal H, Singh T, Singh J, Karmakar S (2013) At-site design rainfall estimation with diagnostic check for nonstationarity: an application to Mumbai rainfall datasets. *Hydro*, IIT Madras, 4–6 December
- Sherly MA, Karmakar S, Chan T, Rau C (2015) Design rainfall framework using multivariate parametric–nonparametric approach. *J Hydrol Eng* 21(1):04015049. [https://doi.org/10.1061/\(ASCE\)HE.1943-5584.0001256](https://doi.org/10.1061/(ASCE)HE.1943-5584.0001256)
- Shyamala B, Bhadrani CVV (2006) Impact of mesoscale-synoptic scale interactions on the Mumbai historical rain event during 26–27 July 2005. *Curr Sci* 91(12):1649–1654 (<https://www.currentscience.ac.in/Volumes/91/12/1649.pdf>). Accessed 20 Nov 2022
- Singh A, Sharma CS, Jeyaseelan AT, Chowdary VM (2015) Spatio-temporal analysis of groundwater resources in Jalandhar district of Punjab state, India. *Sustain Water Resour Manag* 1:293–304. <https://doi.org/10.1007/s40899-015-0022-7>
- Singh O, Kasana A, Singh KP, Sarangi A (2019) Analysis of drivers of trends in groundwater levels under rice–wheat ecosystem in Haryana, India. *Nat Resources Res* 29(2):1101–1126. <https://doi.org/10.1007/s11053-019-09477-6>
- Stowasser M, Annamalai H, Hafner J (2009) Response of the South Asian summer monsoon to global warming: mean and synoptic systems. *J Clim* 22(4):1014–1036. <https://doi.org/10.1038/nclimate1495>
- Tawde SA, Singh C (2015) Investigation of orographic features influencing spatial distribution of rainfall over the Western Ghats of India using satellite data. *Int J Climatol* 35(9):2280–2293. <https://doi.org/10.1002/joc.4146>
- Turner AG, Hannachi A (2010) Is there regime behavior in monsoon convection in the late 20th century? *Geophys Res Lett* 37(16):L16706. <https://doi.org/10.1029/2010GL044159>
- Ueda H, Iwai A, Kuwako K, Hori ME (2006) Impact of anthropogenic forcing on the Asian summer monsoon as simulated by eight GCMs. *Geophys Res Lett* 33(6):L06703. <https://doi.org/10.1029/2005GL025336>
- United Nations (2012) World urbanization prospects: the 2011 revision. New York: United Nations. https://www.un.org/en/development/desa/population/publications/pdf/urbanization/WUP2011_Report.pdf. Accessed 12 June 2022
- Venkatesh B, Jose MK (2007) Identification of homogeneous rainfall regimes in parts of Western Ghats region of Karnataka. *J Earth Sys Sci* 116(4):321–329 (http://wgbis.ces.iisc.ernet.in/biodiversity/sahyadri_eneews/newsletter/issue53/bibliography/26-identification-of-homogenous-rainfall-regimes-%20in-%20parts-of-WG-region-of-Karnataka.pdf). Accessed 14 June 2022
- Vincent LA et al (2005) Observed trends in indices of daily temperature extremes in South America 1960–2000. *J Clim* 18:5011–5023. <https://doi.org/10.1175/JCLI3589.1>
- Vincent LA, Mekis E (2006) Changes in daily and extreme temperature and precipitation indices for Canada over the 20th century. *Atmos Ocean* 44(2):177–193. <https://doi.org/10.3137/ao.440205>
- Warwade P, Tiwari S, Ranjan S, Chandniha SK, Adamowski J (2018) Spatio-temporal variation of rainfall over Bihar State, India. *J Water Land Dev* 36(1):183–197. <https://doi.org/10.2478/jwld-2018-0018>
- Wilby RL, Wigley TML (2002) Future changes in the distribution of daily precipitation totals across North America. *Geophys Res Lett* 29(7):1135. <https://doi.org/10.1029/2001GL013048>
- Winingaard JB, Kleink Tank AMG, Konnen GP (2003) Homogeneity of 20th century European daily temperature and precipitation series. *Int J Climatol* 23:679–692. <https://doi.org/10.1002/joc.906>
- World Bank (2010) Climate risks and adaptation in Asian coastal megacities: a synthesis report. World Bank, Washington DC
- Yang S, Wang XL, Wild M (2018) Homogenization and trend analysis of the 1958–2016 in situ surface solar radiation records in China. *J Climat* 31:4529–4541. <https://doi.org/10.1175/JCLI-D-17-0891.1>

- Yozgatligil C, Yazici C (2016) Comparison of homogeneity tests for temperature using a simulation study. *Int J Climatol* 36:62–81. <https://doi.org/10.1002/joc.4329>
- Zhai P, Zhang X, Wan H, Pan X (2005) Trends in total precipitation and frequency of daily precipitation extremes over China. *J Clim* 18:1096–1108. <https://doi.org/10.1080/19475705.2019.1609604>
- Zhang S, Lu XX, Higgitt DL, Chen CTA, Han J, Sun H (2008) Recent changes of water discharge and sediment load in the Zhujiang (Pearl River) Basin, China. *Global Planetary Change* 60:365–380. <https://doi.org/10.1016/j.gloplacha.2007.04.003>
- Zope PE, Eldho TI, Jothiprakash V (2015) Study of spatio-temporal variations of rainfall pattern in Mumbai city, India. *J Environ Res Develop* 6(2):545–553 (<https://www.semanticscholar.org/paper/STUDY-OF-SPATIO-TEMPORAL-VARIATIONS-OF-RAINFALL-IN-Zope-Eldho/b1c4a9568d463bb3850d746a0ed7cff04b148c5d>)

Publisher's Note Springer Nature remains neutral with regard to jurisdictional claims in published maps and institutional affiliations.

Springer Nature or its licensor (e.g. a society or other partner) holds exclusive rights to this article under a publishing agreement with the author(s) or other rightsholder(s); author self-archiving of the accepted manuscript version of this article is solely governed by the terms of such publishing agreement and applicable law.